AN INVESTIGATION OF EQUIVALENT RADII FOR P_3 CALCULATIONS IN STRONG ABSORBERS

by

LARRY DEAN NOBLE

B. S., Kansas State University, 1961

A MASTER'S THESIS

submitted in partial fulfillment of the

requirements for the degree

MASTER OF SCIENCE

Department of Nuclear Engineering

KANSAS STATE UNIVERSITY
Manhattan, Kansas

1964

Approved by:

John O. Mingle
Major Professor

CONTENTS

NOMENCLATURE

a_1, b_1	Square of the roots of the characteristic equation in the absorber and moderator, respectively
A_1, B_1, C_1	Constants determined from the boundary conditions
D_1	Parameters for empirical fit of total flux
E	Energy, or Least squares error
$f(\underline{r},\underline{\Omega})$	Angular flux
$f_{\ell m}(\underline{r})$	Spherical harmonics component of angular flux
i,j,k,l,m,n	Summation indices
$P_{\ell m}(\underline{\Omega})$	Associated spherical harmonics (see p. 224, reference 24)
$Q(\underline{r},\underline{\Omega})$	Neutron source
$Q_{\ell m}(\underline{r})$	Spherical harmonics component of neutron source
$R_{\ell m}$	Elements of solution vectors
$\underline{r}$	Field position vector
$d\underline{r}$	Differential volume element
r	Distance perpendicular to cylinder axis
s_ℓ	Spherical harmonics component of scattering cross section
T	Matrix containing coefficients of the A_1, B_1, and C_1 as given by the boundary conditions
v	Neutron speed
X	Column matrix containing the A_1, B_1, and C_1
x_1	Elements of X
z	Distance along cylinder axis
$\Sigma\alpha_i, \Sigma\beta_i$	Radial relaxation constants in absorber and moderator, respectively
γ_0	Σ_a/Σ
γ_1	Σ_{tr}/Σ

θ	Angle between $\underline{\Omega}$ and the z- axis
$\Sigma\lambda$	Relaxation constant in z direction
$\bar{\mu}_0$	Average cosine of scattering angle
Σ	Total macroscopic cross section, $\Sigma_a + \Sigma_s$
Σ_a	Macroscopic absorption cross section
Σ_s	Macroscopic scattering cross section
Σ_{tr}	Macroscopic transport cross section, $\Sigma - \bar{\mu}_0 \Sigma_s$
ϕ	Angle between r and the projection of $\underline{\Omega}$ onto a plane perpendicular to the z- axis
$\Phi(r)$	Total neutron flux
$\underline{\Omega}$	Unit vector in the direction of neutron motion
$d\underline{\Omega}$	Differential solid angle

1.0 INTRODUCTION

In the microscopic theory of thermal neutron chain reactors one of the important quantities which must be determined is the thermal utilization (8,24). The thermal utilization depends on the ratio of the number of neutrons absorbed in the moderator to the number absorbed in the fuel. In a homogeneous reactor this ratio is independent of the total flux, Φ, but in heterogeneous reactors it depends on the flux distribution in both the fuel and moderator.

Several methods are used in the determination of the absorption ratio and the suitability of a given method depends, among other things, on the optical thickness of the absorber. For a thin absorber, a "first flight" calculation can be used (14). The neutron blackness, which is defined as the probability that a neutron incident upon a body will be absorbed by it (19), of an absorber depends on the angular distribution of the entrant neutrons and this can be determined only by an exact solution of the transport equation. If the entrant distribution can be approximated as that described by diffusion theory (2), Stuart's blackness chart (18) can be easily used to calculate the ratio of absorption in the moderator to absorption in the fuel. Numerical methods can be used (6), but this is time consuming and each problem must be worked individually.

A simple method for calculating the absorption ratio is to calculate the total flux distribution in the lattice from the diffusion theory unit cell model. As is well known (1,24), the

ratio determined by this method is lower than the experimental ratio. The experimental flux shows a greater depression, both in the fuel and in the immediately surrounding moderator, than does the simple calculation. The use of the P_3 or higher approximations to the one speed transport equation reduces this discrepancy, but does not account for temperature effects (24). Nevertheless, the simple methods, just because they are simple, are widely used. Fictional cross sections are sometimes used to give better results between theory and experiment (26), but it is not clear that cross sections adjusted to give agreement in one lattice will yield agreement in another lattice.

Another "parameter" which could be adjusted to correct for the faults of the simple theory is the dimension of the absorbing medium. By experimentally determining an equivalent radius for different absorbers, moderators, and physical dimensions, a parameter would be available which could be used to give the correct results by the use of a simple calculation. The general usefulness of such a parameter depends on how well the equivalent radius could be predicted, as a function of lattice parameters, from the results of a relatively few experiments.

The theory, including appropriate boundary conditions and computer programs, and the experimental feasibility of obtaining an equivalent radius for the P_3 approximation by making flux measurements in assemblies having exponential z-dependence is the subject matter of this work. A study of this problem for the P_1 approximation is being made by Porath (15).

2.0 THEORY

2.1 The Spherical Harmonics Approximations

Extensive treatment of the Boltzmann equation can be found in many references (4,14,24). In this work only a brief discussion of the general equation is presented; however particular attention is placed on the P_3 approximation to the spherical harmonics component form of the Boltzmann equation in cylindrical geometry. It is assumed that the diffusing medium is homogeneous and isotropic. Only the monoenergetic, time-independent model for neutron transport is studied.

The general Boltzmann integro-differential equation is[1]

$$\frac{1}{v}\frac{\partial f(\underline{r},\underline{\Omega},E,t)}{\partial t} = -\underline{\Omega}\cdot\nabla_r f(\underline{r},\underline{\Omega},E,t) - \Sigma(\underline{r},\underline{\Omega},E,t)f(\underline{r},\underline{\Omega},E,t) + Q(\underline{r},\underline{\Omega},E,t) + \int dE'd\underline{\Omega}' f(\underline{r},\underline{\Omega}',E',t)\Sigma_s(\underline{r},t,E'\to E,\underline{\Omega}'\to\underline{\Omega}) \tag{1}$$

where $f(\underline{r},\underline{\Omega},E,t)d\underline{r}d\underline{\Omega}dE$ is the number of neutrons in the volume element $d\underline{r}$ having energies between E and E + dE whose directions of motion lie in the solid angle $d\underline{\Omega}$ about $\underline{\Omega}$, multiplied by the neutron speed v; $\Sigma_s(\underline{r},t,E\to E',\underline{\Omega}\to\underline{\Omega}')dE'd\underline{\Omega}'$ is the cross section for changing the neutron energy and direction $E,\underline{\Omega}$ into the range dE', $d\underline{\Omega}'$ at E' and $\underline{\Omega}'$ due to collisions; and

$$\Sigma_s(\underline{r},\underline{\Omega},E,t) = \int dE'd\underline{\Omega}'\Sigma_s(\underline{r},t,E'\to E,\underline{\Omega}'\to\underline{\Omega}) \tag{2}$$

is the cross section for any type of scattering.

The first term on the right side of Eq.(1) represents the

---

1 The coordinate system, spherical harmonics, and much of the nomenclature used in this work are the same as those of Weinberg and Wigner (24), and Kofink (12).

losses due to the straight ahead motion of the neutrons. The second term on the right side accounts for losses due to absorption and scattering out of the phase space. The gain of neutrons is represented by the third and fourth terms on the right side of the equation. The third term accounts for all types of sources, and the fourth term accounts for the gain resulting from the scattering of neutrons into the phase space from any other region.

Davison (4), and others (8,14,24), point out that the assumption of a monoenergetic thermal-neutron group can be justified only for slightly absorbing media in regions away from sources and boundaries. This assumption has yielded results which agree reasonably well with experiment, however, even when the above restrictions do not apply (24). The energy-independent thermal neutron group is used throughout the rest of this work.

Using the restrictions that the medium is homogeneous and isotropic and that the system is monoenergetic and time independent, the Boltzmann equation reduces to

$$-\underline{\Omega}\cdot\underline{\nabla}_r f(\underline{r},\underline{\Omega}) - \Sigma f(\underline{r},\underline{\Omega}) + \int d\underline{\Omega}' f(\underline{r},\underline{\Omega}')\Sigma_s(\underline{\Omega}'\to\underline{\Omega}) + q(\underline{r},\underline{\Omega}) = 0 \qquad (3)$$

Only cylindrical geometry is considered, and the coordinate system is the same as that of Weinberg and Wigner (24), and Kofink (12). These coordinates are: the z- axis of the cylinder; the distance r- from the axis of the cylinder; the angle θ between $\underline{\Omega}$ and the z- axis; and the angle ϕ between r- and the projection of $\underline{\Omega}$ in a plane perpendicular to the z- axis.

In this system of coordinates the Boltzmann equation for neutron transport is given by Eq.(4).

$$-\sin\theta\cos\phi\frac{\partial f(r,y,\theta,\phi)}{\partial r}+\frac{\sin\theta\sin\phi}{r}\frac{\partial f(r,y,\theta,\phi)}{\partial\phi}-\cos\theta\frac{\partial f(r,y,\theta,\phi)}{\partial y}$$
$$-\Sigma f(r,y,\theta,\phi)+\int d\Omega' f(r,\Omega')\Sigma_s(\Omega'\to\Omega)+Q(r,\Omega)=0 \qquad (4)$$

Meghreblian and Holmes (14) show that, since the scattering medius is, by assumption, homogeneous and isotropic, the cross section $\Sigma_s(\Omega'\to\Omega)$ can be a function only of the angle θ_0 between Ω' and Ω. This angular dependence can be conveniently represented as a series of spherical harmonics of the first kind (11).

$$\Sigma_s(\Omega'\to\Omega)=\sum_{\ell=0}^{\infty}s_\ell P_\ell(\cos\theta_0) \qquad (5)$$

Using the orthogonality relation

$$\int d\Omega\, P_{\ell m}(\Omega)P^*_{\ell m'}(\Omega)=(-1)^m\int d\Omega\, P_{\ell m}(\Omega)P_{\ell m'}(\Omega)=\frac{4\pi}{2\ell+1}\delta_{\ell\ell'}\delta_{mm'} \qquad (6)$$

the scattering cross section is

$$\Sigma_s=\int d\Omega'\,\Sigma_s(\Omega'\to\Omega)=4\pi s_0 \qquad (7)$$

The average cosine of the scattering angle is given by

$$\bar{\mu}_0=\overline{\cos\theta_0}=\frac{\int d\Omega'\cos\theta_0\,\Sigma_s(\Omega'\to\Omega)}{\int d\Omega'\,\Sigma_s(\Omega'\to\Omega)}=\frac{s_1}{3s_0}=\frac{\Sigma-\Sigma_{tr}}{\Sigma_s} \qquad (8)$$

To realize the full advantage of decomposing the scattering cross section into spherical harmonics, the same is done for the angular flux.

$$f(r,\Omega)=\sum_{\ell=0}^{\infty}\sum_{m=-\ell}^{\ell}f_{\ell m}(r,y)P_{\ell m}(\Omega) \qquad (9)$$

The associated spherical harmonics, $P_{\ell m}(\Omega)$, are the same as those of Weinberg and Wigner (24). The moments are given by

$$f_{\ell m}(r,y)=\frac{2\ell+1}{4\pi}\int d\Omega\, f(r,\Omega)P^*_{\ell m}(\Omega) \qquad (10)$$

The $\ell=0$ and $\ell=1$ terms of Eq.(10) have a simple physical interpretation, but the higher order terms have no simple physical meaning. The total neutron flux at r is obtained by integrating Eq.(9) over all directions Ω. Using the orthogonality relation, the total flux is given by Eq.(11).

$$\Phi(r,z) = \int d\Omega\, f(r,\Omega) = 4\pi f_{00}(r,z) \tag{11}$$

The z- component of the total neutron current is

$$J_z(r,z) = \int d\Omega \cos\theta f(r,\Omega) = \frac{4}{3}\pi f_{10}(r,z) \tag{12}$$

and the r- component of the total neutron current is

$$J_r(r,z) = \int d\Omega \sin\theta \cos\phi f(r,\Omega) = -\frac{4\pi}{3\sqrt{2}}\left[f_{1,1}(r,z) - f_{1,-1}(r,z)\right] \tag{13}$$

To obtain the spherical harmonics component form of the Boltzmann equation, the source term is expanded in terms of the associated spherical harmonics and the addition formula

$$P_\ell(\cos\theta_0) = \sum_{m=-\ell}^{\ell} P_{\ell m}(\Omega) P^*_{\ell m}(\Omega') \tag{14}$$

is used with Eq.(5) and then substituted into Eq.(4). Eq.(9) is substituted into Eq.(4) and the resulting equation is multiplied by $P^*_{\ell m}(\Omega)d\Omega$ and integrated over all Ω. Using the recursion relations

$$\begin{aligned}
\sin\theta\, e^{i\phi} P_{\ell m}(\Omega) &= \left[(2\ell+1)C_{\ell m} P^{m+1}_{\ell-1}(\Omega) - (2\ell+3)A_{\ell m} P^{m+1}_{\ell+1}(\Omega)\right]/(2\ell+1)\\
\sin\theta\, e^{i\phi} P_{\ell m}(\Omega) &= \left[(2\ell+3)B_{\ell m} P^{m-1}_{\ell+1}(\Omega) - (2\ell-1)D_{\ell m} P^{m-1}_{\ell-1}(\Omega)\right]/(2\ell+1)\\
\cos\theta\, P_{\ell m}(\Omega) &= \left[(2\ell+3)E_{\ell m} P^{m}_{\ell+1}(\Omega) + (2\ell-1)F_{\ell m} P^{m}_{\ell-1}(\Omega)\right]/(2\ell+1)
\end{aligned} \tag{15}$$

the spherical harmonics component form of the Boltzmann equation is obtained.

$$\begin{aligned}
&A_{\ell m}\left[\frac{\partial}{\partial r} + \frac{m+1}{r}\right] f^{m+1}_{\ell+1}(r,z) - B_{\ell m}\left[\frac{\partial}{\partial r} - \frac{m-1}{r}\right] f^{m-1}_{\ell+1}(r,z) - C_{\ell m}\left[\frac{\partial}{\partial r} + \frac{m+1}{r}\right] f^{m+1}_{\ell-1}(r,z)\\
&+ D_{\ell m}\left[\frac{\partial}{\partial r} - \frac{m-1}{r}\right] f^{m-1}_{\ell-1}(r,z) - E_{\ell m}\frac{\partial}{\partial z} f^{m}_{\ell+1}(r,z) - F_{\ell m}\frac{\partial}{\partial z} f^{m}_{\ell-1}(r,z)\\
&- \left(\Sigma - \frac{4\pi S_\ell}{2\ell+1}\right) f_{\ell m}(r,z) + Q_{\ell m}(r,z) = 0
\end{aligned} \tag{16}$$

where

$$\begin{aligned}
A_{\ell m} &= \frac{\left[(\ell+m+1)(\ell+m+2)\right]^{1/2}}{2(2\ell+3)} & B_{\ell m} &= \frac{\left[(\ell-m+1)(\ell-m+2)\right]^{1/2}}{2(2\ell+3)}\\
C_{\ell m} &= \frac{\left[(\ell-m-1)(\ell-m)\right]^{1/2}}{2(2\ell-1)} & D_{\ell m} &= \frac{\left[(\ell+m-1)(\ell+m)\right]^{1/2}}{2(2\ell-1)}\\
E_{\ell m} &= \frac{\left[(\ell+m+1)(\ell-m+1)\right]^{1/2}}{2\ell+3} & F_{\ell m} &= \frac{\left[(\ell+m)(\ell-m)\right]^{1/2}}{2\ell-1}
\end{aligned} \tag{17}$$

In the P_L approximation to the spherical harmonics component

form of the Boltzmann equation, it is assumed thal $P_\ell = 0$ for $\ell > L$. For L equal to 1 this assumption leads to the same equations as diffusion theory, but with a different diffusion coefficient.

In the P_1 approximation the total neutron flux is described by a second order differential equation, whereas in the P_3 approximation the total flux must satisfy a fourth order differential equation. The P_3 approximation should give a more accurate description of the total flux in regions rear boundaries, sources, and strong absorbers, where the flux is a rapidly varying function.

2.2 Solutions for Particular Conditions

The spherical harmonics component form of the Boltzmann equation in cylindrical geometry was solved for two different cases. Both cases consist of a two region medium which is radially symmetric. In this work the central region is referred to as the absorber, and the surrounding region as the moderator. A condition of symmetry which must be satisfied for both cases is that there be no current around the z- axis.

The first case, which in this work is called the z-dependent case, is a two region medium having sources at the z = 0 plane and having one surface of the moderator exposed to a vacuum. The second case is the unit cell problem with an isotropic source in the moderator.

In a non-multiplying medium with sources at z = 0, Glasstone and Edlund (9) show, that in regions away from sources and the finite end of the cylinder, the z-dependence of the total neutron flux can be described by a decaying exponential. For this reason, and because of the simplicity of the boundary conditions, it was assumed that the medium extends to infinity in the positive z-direction.

Letting $$\gamma_\ell = 1 - 4\pi S_\ell/[(2\ell+1)\Sigma] \tag{15}$$

and using the assumption

$$f_{\ell m}(r,z) = [C_1 R_{\ell m}(\alpha) I_m(\alpha\Sigma r) + C_2 S_{\ell m}(\alpha) K_m(\alpha\Sigma r)] e^{-\lambda\Sigma z} + [C_3 T_{\ell m}(\alpha) I_m(\alpha\Sigma r) + C_4 U_{\ell m}(\alpha) K_m(\alpha\Sigma r)] e^{\lambda\Sigma z} \tag{16}$$

in Eq.(16), the solution for the z dependent case with linear anisotropic scattering is derived in Appendix A and is given

here for the P_3 approximation.

In the absorber (central region):

$$f_{\ell m}(r,\mu) = \sum_{i=1}^{4} A_i R_{\ell m}(\alpha_i) I_m(\alpha_i r) e^{-\lambda z \mu} \tag{20}$$

In the moderator (surrounding medium):

$$f_{\ell m}(r,\mu) = R_{\ell m}(\beta_1)\left[B_1 J_m(\beta_1 r) + C_1 Y_m(\beta_1 r)\right] e^{-\lambda z \mu} + \sum_{i=2}^{4} R_{\ell m}(\beta_i)\left[B_i I_m(\beta_i r) + (-1)^m C_i K_m(\beta_i r)\right] e^{-\lambda z \mu} \tag{21}$$

Letting

$$g = 1 + \gamma_0\left(\frac{4}{5} + \frac{27}{35}\gamma_1\right) \tag{22}$$

the roots of the characteristic equation in the absorber are

$$\begin{aligned} \lambda^2 + \alpha_1^2 &= \tfrac{35}{18} g\left[1 - (1 - 108\gamma_0\gamma_1/35g^2)^{1/2}\right] = a_1 \\ \lambda^2 + \alpha_2^2 &= \tfrac{35}{18} g\left[1 + (1 - 108\gamma_0\gamma_1/35g^2)^{1/2}\right] = a_2 \\ \lambda^2 + \alpha_3^2 &= 7 \\ \lambda^2 + \alpha_4^2 &= 35\gamma_1/(8\gamma_1 + 7) = a_4 \end{aligned} \tag{23}$$

For $i \neq 1$ the roots of the characteristic equation in the moderator ($\sqrt{b_i}$) are obtained from the above relations by replacing absorber values of γ_0 and γ_1 with moderator values. For $i = 1$

$$\lambda^2 - \beta_1^2 = \tfrac{35}{18} g\left[1 - (1 - 108\gamma_0\gamma_1/35g^2)^{1/2}\right] = b_1 \tag{24}$$

Although there are 8 roots in each region, only the 4 positive values are retained because λ must be positive in order to have a decaying exponential and the Bessel functions of positive argument are not independent of the Bessel functions of negative argument.

The $R_{\ell m}(\alpha_i)$ are given in Table 1. Except for $i = 1$, the $R_{\ell m}(\beta_i)$ are calculated from the same relations by replacing absorber values of γ_0 and γ_1 with moderator values and by replacing α_i with β_i and a_1 with b_1.

Using the relations $\sigma = -i\lambda$, $\nu = \alpha$, $i\bar{a}_{\ell m}\left[(2\ell + 1)/4\pi\right]^{1/2} = R_{\ell m}$ for $\ell + m$ odd, and $a_{\ell m}\left[(2\ell + 1)/4\pi\right]^{1/2} = R_{\ell m}$ for $\ell + m$ even, where

Table 1

Elements of Solution Vectors
for the z-Dependent Case*

ℓ	m	$R_{\ell m}(\alpha_j)$ $j = 1,2$	$R_{\ell m}(\alpha_3)$	$R_{\ell m}(\alpha_4)$
0	0	1	0	0
1	0	$3\gamma_0\lambda/a_j$	0	1
1	1	$3\gamma_0\alpha_j/a_j\sqrt{2}$	0	$-\lambda/\alpha_4\sqrt{2}$
2	0	$(3\lambda^2-a_j)N_j$	1	$5\gamma_1\lambda/a_4$
2	1	$\alpha_j\lambda N_j\sqrt{6}$	$-2\lambda/\alpha_3\sqrt{6}$	$-5(2\lambda^2-a_4)M/\sqrt{6}$
2	2	$\alpha_j^2 N_j\sqrt{6}/2$	$(\lambda^2+7)/\alpha_3^2\sqrt{6}$	$-5\gamma_1\lambda/a_4\sqrt{6}$
3	0	$3\lambda(5\lambda^2-3a_j)N_j/5$	λ	$\gamma_1(5\lambda^2-a_4)/a_4$
3	1	$3\sqrt{3}\alpha_j(5\lambda^2-a_j)N_j/10$	$-(3\lambda^2-7)/2\alpha_3\sqrt{3}$	$-\lambda(15\lambda^2-11a_4)M/2\sqrt{3}$
3	2	$9\lambda\alpha_j^2 N_j/\sqrt{30}$	$\lambda(3\lambda^2-7)/\alpha_3^2\sqrt{30}$	$-5\gamma_1(3\lambda^2-a_4)/a_4\sqrt{30}$
3	3	$3\alpha_j^3 N_j/2\sqrt{5}$	$(\lambda^2+7)/2\alpha_3\sqrt{5}$	$-\sqrt{5}\gamma_1\alpha_4\lambda/2a_4$

$a_j N_j = (a_j-3\gamma_0\gamma_1-7\gamma_0)/(a_j-7)$ $\qquad$ $M = \gamma_1/a_4\alpha_4$

*The $R_{\ell m}(\beta_1)$ are obtained from the $R_{\ell m}(\alpha_1)$ by using moderator values of γ_0 and γ_1, replacing a_1 with b_1, replacing α_1 by β_1 and then multiplying by $(-1)^m$.

i is the square root of -1, the coefficients in Table 1 can be compared with the coefficients in the work performed by Tralli and Agresta (23). In particular; the $R_{32}(\alpha_1)$, $R_{20}(\alpha_4)$, $R_{31}(\alpha_4)$, and $R_{33}(\alpha_4)$ should be compared.

The unit cell model is frequently used in heterogeneous reactor calculations. Some of the assumptions which are called for in this model are; the slowing down density is constant in the moderator and zero in the fuel, the fuel lattice is broken up into a number of identical unit cells, and the fuel elements are so long that the z-dependence of the flux can be neglected.

Using the same notation as was used in the z-dependent case, and assuming that

$$f_{pm}(r) = C_1 P_{pm}(d) I_m(\alpha_1 r) + C_2 S_{pm}(\alpha) K_m(\alpha_1 r) \tag{25}$$

the solution for the unit cell problem with an isotropic source term and linear anisotropic scattering is derived in Appendix A and is given here for the P_3 approximation.

In the absorber:

$$f_{pm}(r) = \sum_{i=1}^{3} A_i P_{pm}(\alpha_i) I_m(\alpha_i r) \tag{26}$$

In the moderator:

$$f_{pm}(r) = \sum_{i=1}^{3} P_{pm}(\beta_i) \left[B_i I_m(\beta_i r) + (-1)^n C_i K_m(\beta_i r) \right] + \frac{Q_{pm}}{\Sigma_a} \delta_{p0} \delta_{m0} \tag{27}$$

Letting $$q = 1 + \gamma_0 \left(\frac{4}{5} + \frac{27}{35} \gamma_1 \right) \tag{22}$$

the roots of the characteristic equation in the absorber are

$$\begin{aligned} \alpha_1^2 &= \tfrac{35}{18} q \left[1 - (1 - 108 \gamma_0 \gamma_1 / 35 q^2)^{1/2} \right] \\ \alpha_2^2 &= \tfrac{35}{18} q \left[1 + (1 - 108 \gamma_0 \gamma_1 / 35 q^2)^{1/2} \right] \\ \alpha_3^2 &= 7 \end{aligned} \tag{28}$$

The α_i are calculated using absorber values of γ_0 and γ_1, and the β_i are calculated from the same equations by using

moderator values of γ_0 and γ_1. As with the z-dependent case, only the positive roots need be retained.

The $R_{\ell m}(\alpha_j)$ are given in Table 2. The $R_{\ell m}(\beta_j)$ are calculated from the same relations by replacing absorber values of γ_0 and γ_1 with moderator values.

Table 2

Elements of Solution Vectors
for the Unit-Cell Model

ℓ	m	$R_{\ell m}(\alpha_j)$ $j = 1,2$	$R_{\ell m}(\alpha_3)$
0	0	1	0
1	1	$3\gamma_0/\alpha_j\sqrt{2}$	0
2	0	$5N_j/4$	1
2	2	$-5N_j\sqrt{6}/8$	$1/\sqrt{6}$
3	1	$3\alpha_j N_j\sqrt{3}/8$	$\alpha_3/2\sqrt{3}$
3	3	$-3\alpha_j N_j\sqrt{5}/8$	$\alpha_3/2\sqrt{5}$

$$N_j = 1 - 3\gamma_0\gamma_1/\alpha_j^2$$

2.3 Boundary Conditions

The exact boundary condition at an interface between media is that the angular flux shall be continuous. This implies that the moments shall be continuous. The exact condition at a free surface is

$$f(\underline{r},\underline{\Omega}) = 0 \qquad \text{for } \underline{\Omega} \text{ inward, } \underline{r} \text{ on the free surface.} \tag{29}$$

In the spherical harmonics component form, an infinite number of terms are required in order to satisfy either of these conditions.

Three methods (4) are generally employed in approximating Eq.(29). The first is collocation wherein $f(\underline{r},\underline{\Omega})$ is made equal to zero at the required number of points $\underline{\Omega}_i$. Next is Mark's boundary condition where one imagines the vacuum to be a medium with zero scattering cross section and requires the angular flux to be continuous. The last consists in employing a set, $Z_{\ell m}(\underline{\Omega})$, which is orthogonal to the angular flux in the region for $\underline{\Omega}$ inward, and then making $\int f(\underline{r},\underline{\Omega}) Z_{\ell m}(\underline{\Omega}) d\underline{\Omega}$ equal to zero for $\underline{r}$ on the free surface and $\underline{\Omega}$ inward. The set of $Z_{\ell m}(\underline{\Omega})$ is usually chosen from the spherical harmonics of odd order ℓ, since this set automatically includes the physical requirement that the inward neutron current is zero. These are called Marshak's boundary conditions and can be expressed as

$$\int f(\underline{r},\underline{\Omega}) P_{\ell m}(\underline{\Omega}) d\underline{\Omega} = 0 \qquad \text{for } \underline{\Omega} \text{ inward, } \underline{r} \text{ on the free surface, all m, } \ell \text{ odd and } \leq L \tag{30}$$

where L is the maximum ℓ in an odd order approximation to the spherical harmonics component form of the Boltzmann equation.

In the P_L approximation, for L less than about 5 or 7, Marshak's boundary conditions lead to the best convergence (4). These are the boundary conditions which were used in this work.

As is shown in Appendix A and as can be seen from the solutions for the $f_{\ell m}(r,z)$, for radial symmetry

$$f_{\ell,-m}(r,z) = (-1)^m f_{\ell,m}(r,z) \tag{31}$$

Using this stipulation, the angular flux for the z-dependent case becomes

$$\begin{aligned} f(r,z,\theta,\phi) &= f_{00}(r,z) + f_{10}(r,z)\cos\theta - f_{11}(r,z)\sqrt{2}\sin\theta\cos\phi \\ &+ f_{20}(r,z)\tfrac{1}{2}(3\cos^2\theta - 1) - f_{21}(r,z)\sqrt{6}\cos\phi\sin\theta\cos\theta + f_{22}(r,z)\tfrac{1}{2}\sqrt{6}\cos 2\phi\sin^2\theta \\ &+ f_{30}(r,z)\tfrac{1}{2}(5\cos^3\theta - 3\cos\theta) - f_{31}(r,z)\tfrac{1}{2}\sqrt{3}\cos\phi\sin\theta(5\cos^2\theta - 1) \\ &+ f_{32}(r,z)\tfrac{1}{2}\sqrt{30}\cos 2\phi\sin^2\theta\cos\theta - f_{33}(r,z)\tfrac{1}{2}\sqrt{5}\cos 3\phi\sin^3\theta \end{aligned} \tag{32}$$

For large R, the outer boundary of the system, Eq.(30) becomes

$$\int_{\pi/2}^{3\pi/2}\int_{0}^{\pi} f(R,z,\Omega)\, P_{\ell m}(\Omega)\sin\theta\, d\theta\, d\phi = 0 \qquad \text{for all m, } \ell \text{ odd and} \leq L. \tag{33}$$

Substituting Eq.(32) into Eq.(33) and performing the indicated integrations

for P_{10}: $$\tfrac{2}{3} f_{00}(R,z) + \tfrac{1}{4}\sqrt{6}\, f_{21}(R,z) = 0 \tag{34-a}$$

for P_{11}: $$f_{00}(R,z) + \tfrac{2}{3}\sqrt{2}\, f_{11}(R,z) - \tfrac{1}{8} f_{20}(R,z) + \tfrac{1}{8}\sqrt{6}\, f_{22}(R,z) = 0 \tag{34-b}$$

for P_{30}: $$-\tfrac{1}{8}\sqrt{6}\, f_{21}(R,z) + \tfrac{4}{7} f_{30}(R,z) = 0 \tag{34-c}$$

for P_{31}: $$\tfrac{1}{4} f_{00}(R,z) + \tfrac{\sqrt{7}}{16} f_{20}(R,z) - \tfrac{1}{48}\sqrt{6}\, f_{22}(R,z) + \tfrac{8}{21}\sqrt{3}\, f_{31}(R,z) = 0 \tag{34-d}$$

for P_{32}: $$\tfrac{1}{8}\sqrt{6}\, f_{21}(R,z) + \tfrac{4}{33}\sqrt{30}\, f_{32}(R,z) = 0 \tag{34-e}$$

for P_{33}: $$-\tfrac{1}{4} f_{00}(R,z) + \tfrac{1}{16} f_{20}(R,z) + \tfrac{3}{16}\sqrt{6}\, f_{22}(R,z) + \tfrac{8}{33}\sqrt{5}\, f_{33}(R,z) = 0 \tag{34-f}$$

Davison (4) shows that the number of conditions which need to be satisfied at a free surface is equal to the number of even order moments, N(ℓ=even), and the conditions to be satisfied at an interface between media is 2N(ℓ=even). The use of either

Marshak's boundary conditions or the requirement that the angular flux shall be continuous introduces N(ℓ=odd) - N(ℓ=even)' excess conditions.

Most applications of the spherical harmonics method have been to cases where the number of odd order moments was equal to the number of even order moments. For cases in which the number of odd order moments is greater than the number of even order moments, Davison (4) suggests, by means of an intuitive argument, that it should be better to make the moments for all m with $\ell \leq$ L-1 continuous first and then to make the "predominately normal" moments of order L continuous. The same consideration should apply to the choice of the $P_{\ell m}(\underline{\Omega})$ in Eq.(33).

The above problem does not arise in the unit cell problem. Since the z-dependence is neglected, the angular flux should be symmetric about any plane perpendicular to the z- axis. This means that

$$f(r, \theta, \phi) = f(r, \pi-\theta, \phi) \tag{35}$$

From an inspection of Eq.(32) it is seen that this condition can be satisfied if only such $f_{\ell m}(r)$ are retained as have $\ell + m$ even.

In addition to the requirement that the angular flux shall be continuous at the interface, the usual condition used in the unit cell problem is that the angular flux shall be symmetric about the cell boundary R_c. That is,

$$f(R_c, \theta, \phi) = f(R_c, \theta, \pi-\phi) \tag{36}$$

Since only the $f_{\ell m}(r)$ with $\ell + m$ even are retained, an inspection of Eq.(32) shows that this condition can be satisfied if it is required that Eq.(37) be satisfied.

$$f_{11}(R_c) = f_{31}(R_c) = f_{33}(R_c) = 0 \qquad (37)$$

It is noted that the number of even order moments is equal to the number of odd order moments so that the number of boundary conditions is equal to the number of unknowns.

3.0 DISCUSSION AND RESULTS

3.1 Consideration of Boundary Conditions

In order to apply the equations which have been derived for the P_3 approximation to the z-dependent case, an appropriate choice of boundary conditions must be made. For a two region problem with known cross sections and dimensions, Eqn's (20),(21), and (23) show that there are 13 unknowns which must be determined; λ and 4 each of the A_1, B_1, and C_1. It was shown that there are a total of 17 available boundary conditions; 10 from the requirement that the angular flux be continuous at the interface, 6 from Marshak's boundary conditions at the free surface, and 1 from the source condition. In order to have a meaningful solution, one of the unknowns, say A_1, must be determined by the source condition. This leaves 12 unknowns to be determined from 16 equations. Of these 16, any 8 of the 10 obtained by matching moments at the interface plus any 4 of the 6 obtained from Marshak's conditions form an appropriate set of 12 equations in 12 unknowns.

Two procedures for solving the set of 16 equations are to select the "best" 12 equations or to retain all 16 equations and minimize the error in some manner. Most work with the P_3 approximation has been to cases where the number of available equations is equal to the number of unknowns (3,12), and as far as is known to the author, no extensive effort has been made to determine which equations should be used when there are excess equations. As mentioned previously, Davison (4) gives an intuitive argument for the appropriate choice. Tralli and Agresta (23) treat a

problem similar to the previously described unit cell model except that they consider a finite cylinder. For their problem there are 12 unknowns and 14 equations. They retain all 14 equations. Which of the two procedures gives the better approximation to the exact solution of the transport equation is not known, however it is much easier, and is consistent with the method used in the P_1 approximation, to choose the "best" boundary conditions.

Any appropriately chosen combination of the 12 homogeneous equations can be solved by arranging the equations so that the following matrix equation applies.

$$TX = 0 \tag{38}$$

Where X is a column matrix containing the A_i, B_i, and C_i, and T is a square matrix containing the coefficients of the unknowns as given by the 12 equations. In principal, the application of Cramer's Rule and the reduction of the determinant yields an explicit equation for the λ which make the determinant of T equal to zero. Because of the oscillatory nature of the $J_m(r)$ and $Y_m(r)$, there may be an infinite number of these λ_K. For each value of λ, any 11 of the 12 equations can, in principal, be used to determine all the x_i in terms of one of the x_i, say A_1. The complete solution is then the sum of all these solutions, and for the z-dependent case has the following form:

In the absorber:

$$f_{gm}(r,z) = \sum_{K=1}^{\infty} \sum_{i=1}^{4} A_i^K R_{gm}(\alpha_i^K) I_m(\alpha_i^K \Sigma r)\, e^{-\lambda_K \Sigma z} \tag{39}$$

In the moderator:

$$\begin{aligned} f_{gm}(r,z) = {} & \sum_{K=1}^{\infty} R_{gm}(\beta_1^K)\left[\theta_1^K J_m(\beta_1^K \Sigma r) + C_1^K Y_m(\beta_1^K \Sigma r)\right] e^{-\lambda_K \Sigma z} \\ & + \sum_{K=1}^{\infty} \sum_{i=2}^{4} R_{gm}(\beta_i^K)\left[\theta_i^K I_m(\beta_i^K \Sigma r) + (-1)^m C_i^K K_m(\beta_i^K \Sigma r)\right] e^{-\lambda_K \Sigma z} \end{aligned} \tag{40}$$

where the R_{lm}, α, and β are determined from the same relations as before, and the λ_k, as well as the A_1^k, B_1^k, and C_1^k in terms of A_1^k, are determined from the "best" boundary conditions. The only unknowns in the above equations are the A_1^k and these can be determined from the source condition, or equivalently from the specification of the flux at some position.

In order to get some idea as to which boundary conditions should be used, the problem was, at first, simplified by considering a one region medium having a free surface, and containing the origin. For this problem the complete solution is Eq.(40) if the C_1^k are set equal to zero. Knowing B_1^k from the source condition, λ_k and the remainder of the B_1^k are then determined from Marshak's boundary conditions. This reduces the number of possible combinations of boundary conditions to 15.

Instead of considering all 15 possibilities however, it was seen, by reasoning along the lines suggested by Davison (4), that any combination which includes the equation resulting from the use of P_{30} in Marshak's boundary conditions, Eq.(30), should give a poor approximation to the requirement that the inward angular flux be zero, because f_{30} is the predominately "tangential moment" of order 3. This supposition was checked by using what was considered to be one of the better combinations using the P_{30}. This was called Case 1 and used the equations resulting from the use of P_{10}, P_{11}, P_{30}, and P_{31} in Eq.(33). By comparing Fig. 1 with Fig. 8 it was seen that Case 1 gives a much poorer approximation to the desired condition than does the P_1 approximation. Thus, all combinations containing Eq.(34-c) were tentatively rejected.

Of the remaining 5 combinations, one does not contain the equation resulting from the use of P_{11}. This combination defeats the purpose of Marshak's boundary conditions because it no longer contains the stipulation that the inward neutron current be zero. Of the remaining 4 combinations, the results obtained using the P_{10}, P_{11}, P_{31}, and P_{32} in Eq.(33) should be similar to the results obtained by the use of the P_{10}, P_{11}, P_{32}, and P_{33}, since the f_{31} and f_{33} are the "most normal moments" of order 3.

In view of the above considerations, 3 additional combinations of the P_{fm} were used in Eq.(33). These are; Case 2, the P_{10}, P_{11}, P_{31}, and P_{33}; Case 3, the P_{10}, P_{11}, P_{32}, and P_{33}; Case 4, the P_{11}, P_{31}, P_{32}, and P_{33}. In all 4 cases only the first harmonic in Eq.(40) was used, and for every calculation, B_1^1 was arbitrarily set equal to 1000.0. Two different media were studied, iron which has a reasonably large absorption cross section, and graphite which has a small absorption cross section. Radial dimensions of 25.0 and 35.81 mean free paths, ΣR, were used. The cross sections used are listed in Table 3.

Table 3

Cross Sections Used in
Study of Boundary Conditions

Medium	$\Sigma_a (cm^{-1})$	$\Sigma_s (cm^{-1})$	$\Sigma_{tr} (cm^{-1})$
Iron	0.222	0.933	1.144
Graphite	2.83×10^{-4}	0.404	0.381

Some of the results are shown in Figures 1 through 8. The angular flux at the boundary is plotted as a function of ϕ for

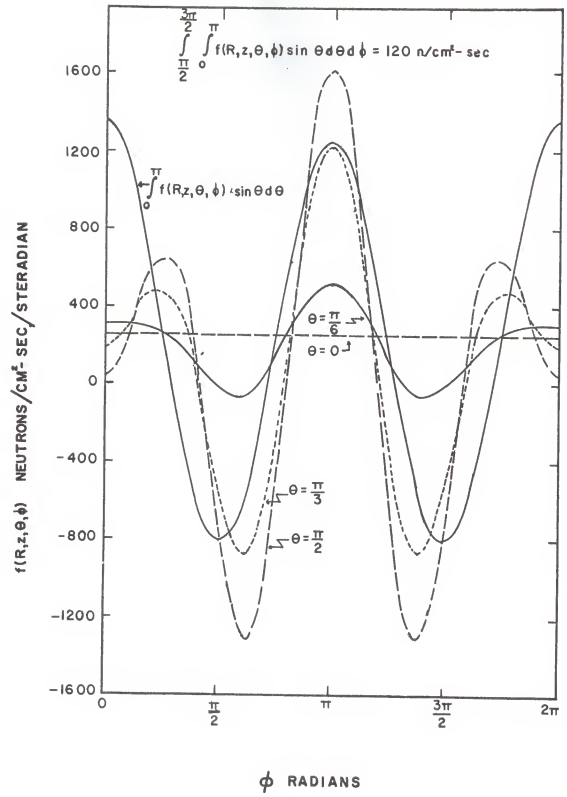

FIG. I CASE I (GRAPHITE, $\Sigma R = 35.81$)

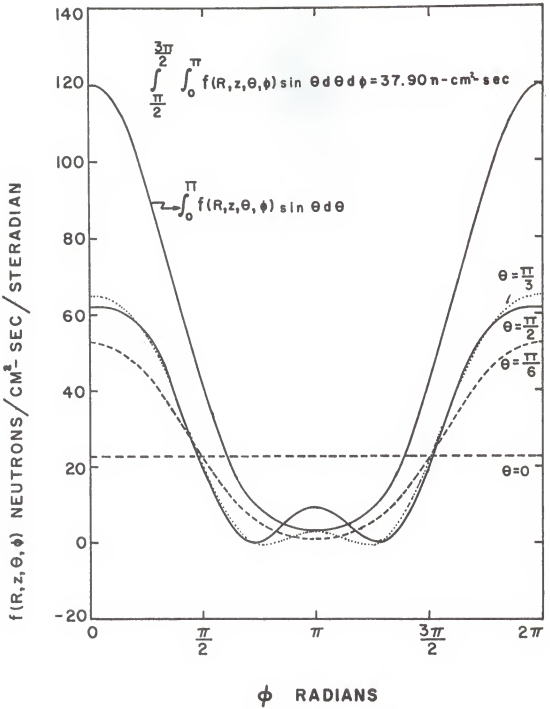

FIG. 2 CASE 2 (GRAPHITE, $\Sigma R = 35.81$)

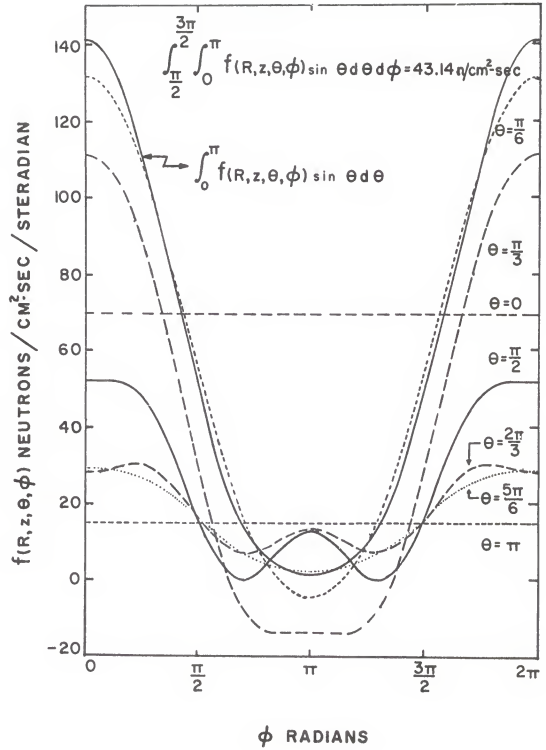

FIG. 3 CASE 2 (IRON, $\Sigma R = 35.81$)

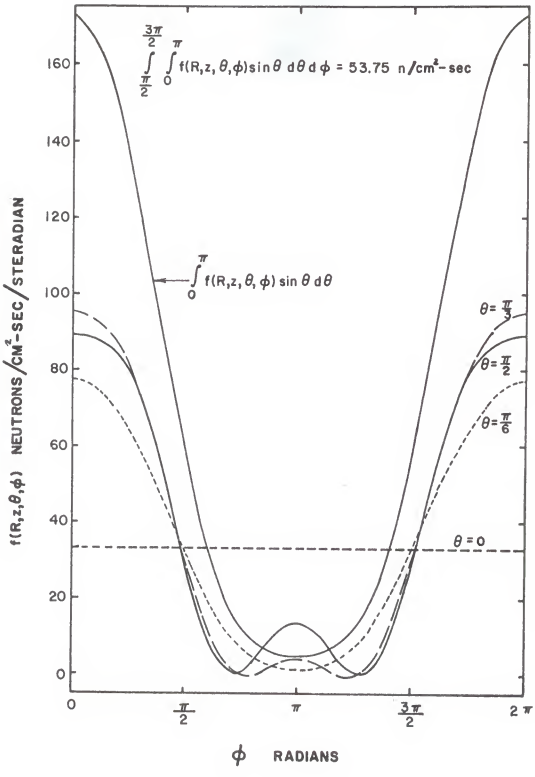

FIG. 4 CASE2 (GRAPHITE, $\Sigma R = 25.0$)

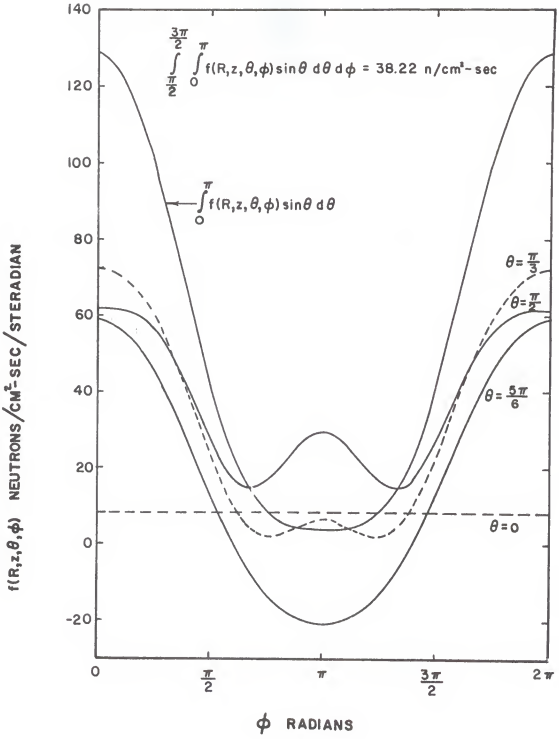

FIG. 5 CASE 3 (GRAPHITE, $\Sigma R = 35.81$)

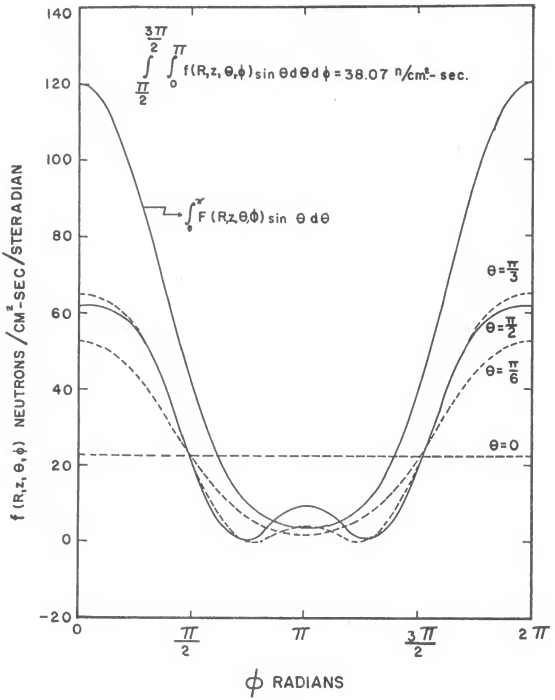

FIG. 6 CASE 4 (GRAPHITE, $\Sigma R = 35.81$)

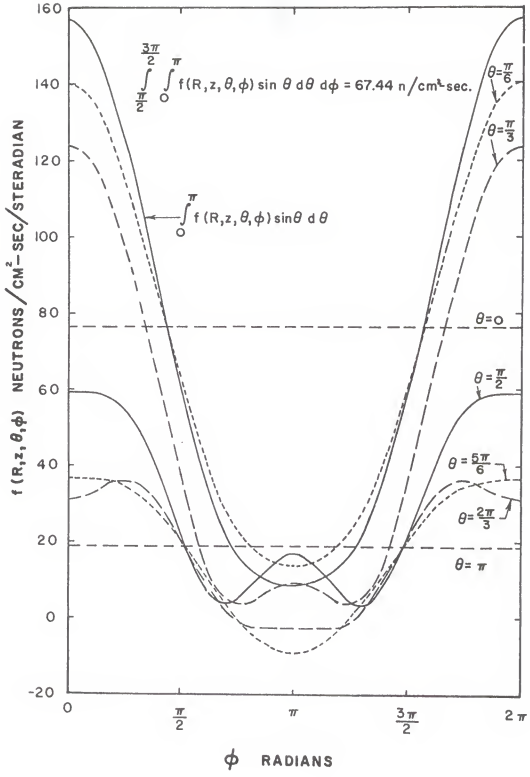

FIG. 7 CASE 4 (IRON, $\Sigma R = 35.81$)

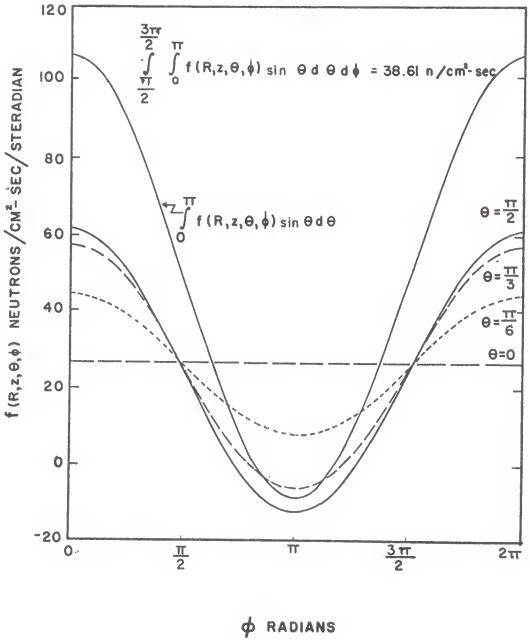

FIG. 8 P_1 APPROXIMATION (GRAPHITE, ΣR=35.81)

various values of θ. In addition, the figures contain a curve for which the θ-dependence of the angular flux has been removed by integration over the θ-dependence of $\underline{\Omega}$. This curve is

$$\int_0^{\pi} f(R,z,\theta,\phi)\sin\theta\,d\theta = 2f_{00}(R,z) - \frac{\pi}{\sqrt{2}}f_{11}(R,z)\cos\phi + \frac{2}{3}\sqrt{5}\,f_{22}(R,z)\cos 2\phi - \sqrt{3}\,\frac{\pi}{16}f_{31}(R,z)\cos\phi - \sqrt{5}\,\frac{3}{16}\pi f_{33}(R,z)\cos 3\phi \tag{41}$$

where R is the radius of the outer boundary and Eq.(32) has been substituted into the integrand. Since the integral of sine from 0 to π is equal to 2, Eq.(41) is also equal to twice the angular flux averaged over the θ-dependence of $\underline{\Omega}$. Also given in the figures is the partial inward flux

$$\int_{\pi/2}^{3\pi/2}\int_0^{\pi} f(R,z,\theta,\phi)\sin\theta\,d\theta\,d\phi = 2\pi f_{00}(R,z) + \sqrt{2}\,\pi f_{11}(R,z) + \sqrt{3}\,\frac{\pi}{8}f_{31}(R,z) - \sqrt{5}\,\frac{\pi}{8}f_{33}(R,z) \tag{42}$$

The parametric dependence of $f(R,z,\theta,\phi)$ with θ for $\theta > \pi/2$ is shown only in Fig. 3 and 7, the cases where iron was the medium under consideration, because the angular flux is almost symmetric about $\theta = \pi/2$ for the graphite medium. There was a slight decrease in the graphite angular flux for $\theta > \pi/2$, but it was small. The B_1 and the value of λ which describe these curves are given in Table 4.

These curves clearly eliminated Case 1 from further consideration and possibly indicated that Case 3 should be rejected also. Cases 2 and 4 appear to satisfy the condition that the angular flux should be zero for $\underline{\Omega}$ inward about equally well.

In order to proceed further it was necessary to consider the two region problem and thus to make a choice of which 8 moments should be matched at the interface. Since Davison's (4) suggestion (Case 2) gave good results at the free surface, his

Table 4

Constants Used in Figures 1 Through 8

$B_1 = 1000.0$

Fig.	B_2	B_3	B_4	λ
1	-1.405×10^{-25}	-9.983×10^{-20}	9.462×10^{-36}	0.074597
2	-1.733×10^{-27}	-1.302×10^{-21}	-4.601×10^{-40}	0.079432
3	-2.586×10^{-28}	-1.806×10^{-18}	1.208×10^{-36}	0.70001
4	-3.776×10^{-18}	-2.373×10^{-14}	-1.337×10^{-27}	0.10347
5	-3.363×10^{-27}	-3.741×10^{-21}	-1.840×10^{-37}	0.079375
6	-1.745×10^{-27}	1.651×10^{-21}	-1.049×10^{-39}	0.079431
7	-5.546×10^{-28}	3.262×10^{-18}	-9.174×10^{-37}	0.69998
8	0.0	0.0	0.0	0.079498

suggestion for which moments to match at the interface was heavily relied upon. As previously mentioned, he suggests that all moments having $\ell \leq L-1$ plus the predominately normal moments of order L be matched at the interface.

The results of Case 2 indicate that the moments of order 3 which should be considered are the f_{31} and f_{33}. Case 3 indicates that the f_{32} and f_{33} should be considered, while Case 4 suggests the f_{31}, f_{32}, and f_{33}. Neither Case 2 nor Case 3 conflicts with Davison's suggestion concerning the 6 moments having $\ell \leq 2$, but Case 4 does. Since the spherical harmonics used in Case 4 all contain at least some normal component, all "normal moments" were matched first and then the remaining moments, starting with $\ell = 0$ until the required number of equations were obtained. Thus, the

f_{20} and f_{30} were not made equal at the interface for Case 4.

Using these rules for Cases 2, 3, and 4, the total neutron flux distribution, $\bar{\Phi}$, was calculated for a central region of iron and a surrounding region of graphite. The cross sections of Table 3 were used.

The distribution calculated for Case 3 was completely unrealistic, peaking very sharply right at the interface, and Case 3 was eliminated. The distribution for Cases 2 and 4 are shown in Fig. 9.

It was seen that there is nothing in Fig. 9 which indicates a preference between Cases 2 and 4. To obtain a better comparison, the angular flux distribution at the interface was calculated with the computer program described in Appendix C. A rod radius of 2.54 cm, moderator radius of 50.0 cm, and the cross sections of Table 3 were used. Only one harmonic was used and A_1 was arbitrarly set equal to 1.0. The results are listed in Tables 5 and 6. As is shown in Appendix A, $f(r,z,\theta,\phi) = f(r,z,\theta,-\phi)$, therefore only values for ϕ between 0 and π are listed.

This calculation clearly showed that Case 2 gives a better approximation to the requirement that the angular flux be continuous at the interface. Therefore, Case 2, which constitutes the equations suggested by Davison (4), were used in the remainder of this work.

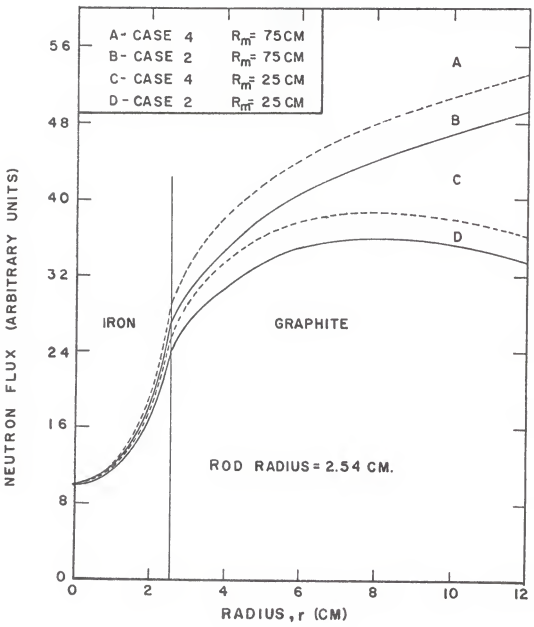

FIG. 9 NEUTRON FLUX AS A FUNCTION OF r FOR TWO DIFFERENT BOUNDARY CONDITIONS.

Table 5

Angular Flux at Interface for Case 2

θ degrees	ϕ degrees	f(moderator) (n/cm^2-sec/ steradian)	f(absorber) (n/cm^2-sec/ steradian)	difference (n/cm^2-sec/ steradian)
0	all values	2.923	2.905	0.018
30	0	1.692	1.741	-0.049
	18	1.756	1.795	-0.039
	36	1.947	1.958	-0.011
	54	2.251	2.228	0.023
	72	2.635	2.584	0.051
	90	3.040	2.978	0.062
	108	3.400	3.349	0.051
	126	3.666	3.643	0.023
	144	3.824	3.835	-0.011
	162	3.897	3.936	-0.039
	180	3.917	3.966	-0.049
60	0	1.387	1.492	-0.105
	18	1.432	1.518	-0.086
	36	1.602	1.640	-0.038
	54	1.960	1.938	0.022
	72	2.507	2.438	0.069
	90	3.134	3.046	0.088
	108	3.658	3.588	0.070
	126	3.935	3.914	0.021
	144	3.960	3.998	-0.038
	162	3.860	3.949	-0.086
	180	3.802	3.906	-0.104
90	0	1.606	1.606	0.0
	18	1.587	1.587	0.0
	36	1.604	1.604	0.0
	54	1.808	1.808	0.0
	72	2.273	2.273	0.0
	90	2.893	2.893	0.0
	108	3.435	3.435	0.0
	126	3.692	3.692	0.0
	144	3.640	3.640	0.0
	162	3.450	3.450	0.0
	180	3.352	3.352	0.0

Table 5 (continued)

θ degrees	ø degrees	f(moderator) (n/cm^2-sec/ steradian)	f(absorber) (n/cm^2-sec/ steradian)	difference (n/cm^2-sec/ steradian)
120	0	1.478	1.373	0.105
	18	1.465	1.379	0.086
	36	1.480	1.442	0.038
	54	1.632	1.654	-0.022
	72	1.986	2.055	-0.069
	90	2.480	2.568	-0.088
	108	2.959	3.028	-0.069
	126	3.271	3.292	-0.021
	144	3.373	3.335	0.038
	162	3.346	3.260	0.086
	180	3.318	3.214	0.104
150	0	1.431	1.382	0.049
	18	1.457	1.418	0.039
	36	1.540	1.529	0.011
	54	1.700	1.723	-0.023
	72	1.937	1.988	-0.051
	90	2.228	2.290	-0.062
	108	2.525	2.576	-0.051
	126	2.777	2.800	-0.023
	144	2.953	2.942	0.011
	162	3.051	3.012	0.039
	180	3.082	3.032	0.050
180	all values	2.172	2.190	-0.018

Table 6

Angular Flux at Interface for Case 4

θ degrees	ϕ degrees	f(moderator) (n/cm^2-sec/ steradian)	f(absorber) (n/cm^2-sec/ steradian)	difference (n/cm^2-sec/ steradian)
0	all values	2.357	4.129	-1.772
30	0	0.667	1.716	-1.049
	18	0.767	1.816	-1.049
	36	1.062	2.110	-1.048
	54	1.527	2.575	-1.048
	72	2.115	3.164	-1.049
	90	2.757	3.805	-1.048
	108	3.368	4.417	-1.049
	126	3.880	4.928	-1.048
	144	4.249	5.297	-1.048
	162	4.465	5.514	-1.049
	180	4.536	5.585	-1.049
60	0	1.618	1.335	0.283
	18	1.675	1.392	0.283
	36	1.870	1.586	0.284
	54	2.243	1.959	0.284
	72	2.785	2.502	0.283
	90	3.403	3.120	0.283
	108	3.947	3.663	0.284
	126	4.295	4.011	0.284
	144	4.427	4.144	0.283
	162	4.427	4.144	0.283
	180	4.410	4.127	0.283
90	0	2.646	1.858	0.788
	18	2.627	1.839	0.788
	36	2.623	1.836	0.787
	54	2.743	1.955	0.788
	72	3.036	2.248	0.788
	90	3.425	2.638	0.787
	108	3.742	2.955	0.787
	126	3.845	3.057	0.788
	144	3.729	2.942	0.787
	162	3.536	2.748	0.788
	180	3.444	2.657	0.787

Table 6 (continued)

θ degrees	ϕ degrees	f(moderator) (n/cm^2-sec/ steradian)	f(absorber) (n/cm^2-sec/ steradian)	difference (n/cm^2-sec/ steradian)
120	0	1.412	1.302	0.110
	18	1.438	1.328	0.110
	36	1.548	1.438	0.110
	54	1.806	1.696	0.110
	72	2.233	2.122	0.111
	90	2.760	2.649	0.111
	108	3.252	3.141	0.111
	126	3.588	3.477	0.111
	144	3.733	3.623	0.110
	162	3.753	3.642	0.111
	180	3.744	3.634	0.110
150	0	0.291	1.211	-0.920
	18	0.369	1.289	-0.920
	36	0.600	1.520	-0.920
	54	0.977	1.897	-0.920
	72	1.472	2.392	-0.920
	90	2.031	2.951	-0.920
	108	2.583	3.503	-0.920
	126	3.060	3.980	-0.920
	144	3.415	4.335	-0.920
	162	3.629	4.549	-0.920
	180	3.700	4.620	-0.920
180	all values	1.743	3.120	-1.377

3.2 Practical Solutions

The most difficult practical problem encountered in the use of the P_3 approximation to the Boltzmann equation for neutron transport in the z-dependent case is the solution of the matrix equation, Eq.(38). In the z-dependent case the determinant of T must be set equal to zero and the λ_κ determined before the x_1^k can be determined in terms of, say, x_1^k. This problem is not encountered in unit cell calculations, because λ is zero and the equations resulting from the application of the boundary conditions are inhomogeneous. Even in the one region z-dependent problem, however, T is a 4x4 matrix, each term of which is a complicated function of λ, and to expand the determinant to obtain the characteristic equation for λ does not appear profitable. A trial and error procedure using hand calculation methods is also out of the question. In the two region problem 16 different Bessel functions, some having as many as 10 different arguments, the various $R_{\ell m}$, plus the value of the 12x12 determinant must be determined for each trial.

The computer programs described in Appendices C and D use a linear interpolation procedure to select succeeding values of λ in an attempt to make the determinant of T equal to zero. The "round off error" in the calculation of a 12x12 determinant can be significant, and it was found that the matrix had to be ordered so that each diagonal element was at least of the same order of magnitude as the largest element in the same column. This was particularly important for the equations at the outer boundary.

Because the dimensions of the moderator were large, the equations at the outer boundary contained both very large and very small numbers (the I_m and K_m of large argument).

Considerable round off was encountered regardless of how the matrix was ordered, and a special subroutine was developed which expanded the numbers to 18 digits, performed the determinant or matrix calculations, and then reduced the answers to 8 digits for further use in the program. This eliminated the large errors which had occurred with the 8 digit arithmetic.

It was not expected that the value of the determinant could be made exactly equal to zero, however the magnitude of the error was quite unexpected. The results of a typical calculation are shown in Table 7, where the "slope" is defined as the rate of change of the determinant of T with λ.

Table 7

The Determination of Lambda

Determinant of T	Slope	$\lambda x10^2$
$3.210x10^{80}$		9.0000000
$-3.394x10^{80}$	$-6.604x10^{82}$	10.000000
$-6.753x10^{78}$	$-6.473x10^{82}$	9.4861780
$1.817x10^{77}$	$-6.647x10^{82}$	9.4757459
$-1.228x10^{74}$	$-6.653x10^{82}$	9.4760192
$5.629x10^{73}$	$-1.791x10^{83}$	9.4760191

It is seen from the table that the best λ obtainable still leaves the magnitude of the determinant quite large. The slope

is very large, however, and the determinant changes sign when the 'best' λ is changed by the smallest available increment. For all practical purposes, then, this 'best' λ is probably the correct λ.

If the determinant of T were exactly equal to zero it would make no difference which 11 of the 12 equations were used to determine the x_i in terms of x_1. Since the determinant was not zero, x_1 was arbitrarly set equal to 1.0, each of the 12 equations were deleted in turn, and the x_1 were calculated from the remaining equations.

The maximum difference in any one of the x_1 was approximately 1 in the fourth digit, and this occurred in only one case and for only one x_1. The maximum difference in the calculated total flux, Φ, at any position was approximately 5 in the seventh digit. This error is probably less than the error due to round off in the rest of the program.

Since the values of the x_1 are, for the purposes of this work (the accuracy in Φ is more important here), independent of which 11 equations are used to determine them, the 'best' value of λ was taken to be the correct value.

3.3 Application of Theory

It is well known (1,8,24) that the P_3 approximation to the Boltzmann equation for neutron transport does not predict as large a total flux depression in an absorber as does the exact solution to the transport equation. One way of increasing the depression in the P_L approximation is to use a fictional absorber dimension which is larger than the actual dimension by an amount just large enough to give the same ratio of average moderator total flux to absorber total flux as is given by the exact solution. What is more important, from the practical point of view, is to find an equivalent radius such that the total flux described by the P_L approximation describes the actual distribution found in a real medium, irregardless of whether or not the actual distribution is described by the exact solution of the transport equation.

The method proposed in this work for finding this equivalent radius is to find the radius which makes the theoretical expression fit the experimental points as accurately as possible. A computer program which is described in Appendix D was developed for this purpose. The fit is made by a trial and error procedure which strives to minimize the sum of the weighted squares of the residuals between the theoretical expression and the experimental values. The weighting factor is the reciprocal of the standard deviation squared (22).

In order to test this program, experimental points in and near an iron rod embedded in a graphite medium were obtained by a

procedure and with the appartus described in Appendix B. These points were not intended to give an accurate description of the neutron flux and several correction factors were neglected. Foulke (7) gives a description of these factors, and only a summary of some of these effects is given here.

A hardening of the neutron spectrum occurs in the iron rod due to preferential absorption of the low energy neutrons in the outer regions of the rod.

Unequal activation on different sides of the foils can occur since foils are seldom thin for neutrons or for the electrons produced by the induced radioactivity. The difference in activity on two sides of a foil depends on the flux gradient near the foil. As can be seen from Figures 1 through 8, this effect should be more pronounced in and near the iron rod if the foil is placed perpendicular to the z- axis.

A foil depresses the flux in a region around itself and since the foils in this experiment were part of a continuous strip of gold, the activity induced at any point in the strip was influenced by the presence of the rest of the strip.

Since gold has a large resonance at about 5 ev, the average energy of the flux which induces the activity is slightly different than the average energy of the neutrons present in the system.

In addition to the errors introduced by the neglect of these corrections, other errors were introduced from an unknown source. A hump in the neutron flux appeared approximately two inches from the edge of the rod in every activation and the cause of this hump is unknown.

The results obtained by fitting the theoretical expression to data taken from Table B-1 is shown in Figures 10 through 15. The effect of the errors mentioned above on these results is probably much less than the effect caused by the use of an iron absorption cross section which was much too large (see Appendix B). Figures 10, 12, and 14 show the best fit obtained by using 1, 2, and 3 harmonics, along with the equivalent radii which resulted. Fig. 11 illustrates the relative effects of using 1, 2, and 3 harmonics for the actual rod radius of 0.5 in. Higher harmonics would presumably give better results, but three harmonics should be sufficient if the measurements are not made too close to the source. Fig. 15, which uses only the data out to the hump mentioned above, illustrates the type of fit which might be expected from a good analysis of an equivalent radius. The fact that the fit is so good in this case appears to be the chance result of a lot of compensating errors.

It is to be noted that the A_1^k of Eq.(39), which describe the curves in the above mentioned figures, were determined solely on the basis of how well the resulting expression for the total flux fit the experimental points. They therefore presumably have no relation to the A_1^k which would be determined by a source condition.

The cross sections and moderator radius which were used to obtain these fits are discussed in Appendix B. No extensive study of the change in equivalent rod radius as a function of cross sections was made. However, the graphite absorption cross section was increased from 2.53×10^{-4} cm^{-1} to 8.6×10^{-4} cm^{-1} and

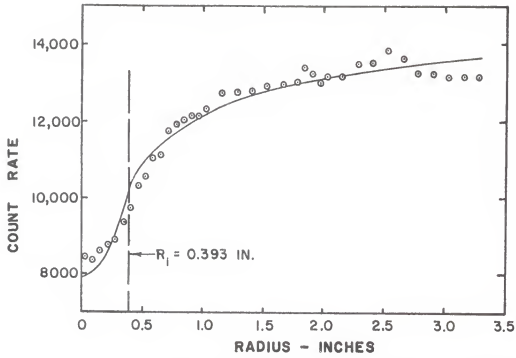

FIG. 10 BEST LEAST SQUARES FIT USING 1 HARMONIC. BEST RADIUS = 0.393 IN.

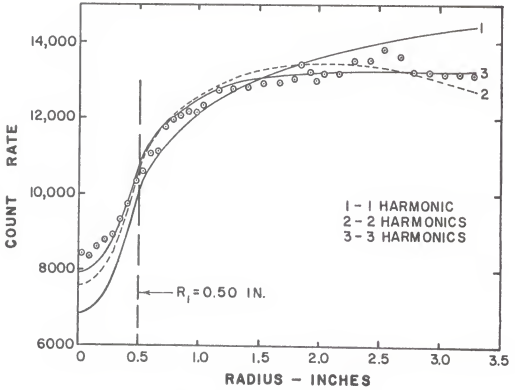

FIG. 11 COMPARISON OF 1, 2, AND 3 HARMONICS USING ACTUAL ROD RADIUS OF 0.5 IN.

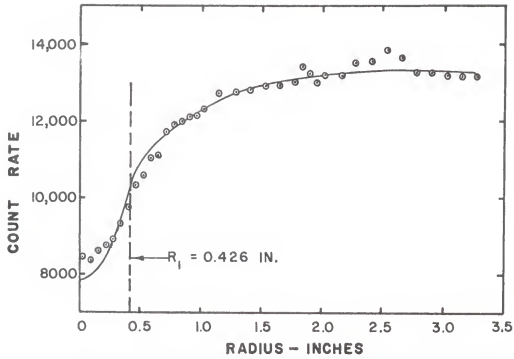

FIG. 12 BEST LEAST SQUARES FIT USING 2 HARMONICS. BEST RADIUS= 0.426 IN.

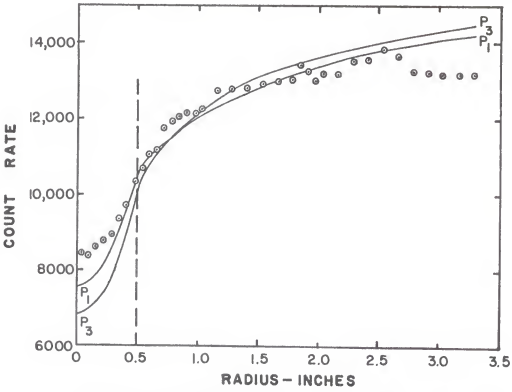

FIG. 13 COMPARISON OF 1 HARMONIC P_1 AND P_3 APPROXIMATIONS USING ACTUAL ROD RADIUS.

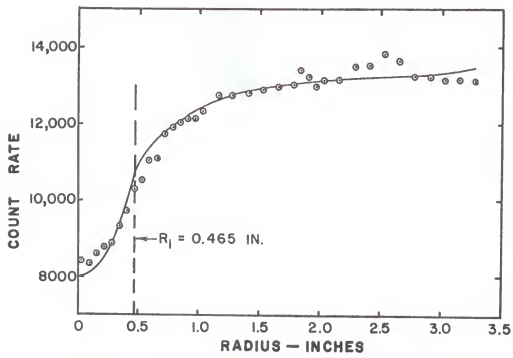

FIG. 14 BEST LEAST SQUARES FIT USING 3 HARMONICS. BEST RADIUS = 0.465 IN.

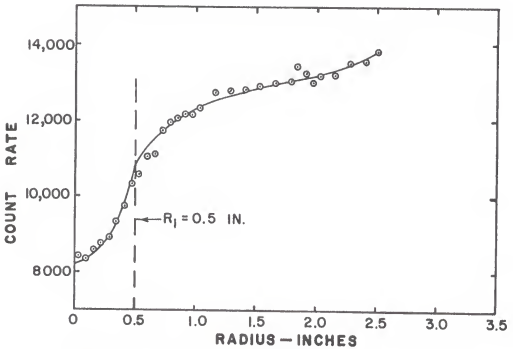

FIG. 15 LEAST SQUARES FIT USING 3 HARMONICS, ONLY 31 DATA POINTS, AND ACTUAL ROD RADIUS.

the resulting increase in the 1 harmonic equivalent rod radius was only 0.4%. A rough estimate of the effect of changes in the iron absorption cross section can be obtained by the use of the P_1 approximation and Fig. 13.

The ratio of the flux at the edge of the rod to the flux at the center is 1.40 for the P_1 approximation shown in Fig. 13. This is the same ratio as predicted by the P_1 approximation for the unit cell model using the same Σ_a of 0.259 cm^{-1}. The experimental flux ratio in Fig. 13 is about 1.27. Other factors remaining constant, the absorption cross section would have to be reduced to 0.17 cm^{-1} in order for the P_1 unit cell model to give the same ratio. Even if the actual iron absorption cross section (0.229 cm^{-1}) had been corrected to an effective neutron temperature (14) and used in these calculations it is doubtful if the 1 harmonic equivalent radius would have been as large as the actual rod radius. It is quite possible, however, that the 3 harmonic radius would have been at least as large as the true rod radius.

3.4 Conclusions

When the P_3 approximation to the Boltzmann equation for neutron transport is used in cylindrical geometry which does not have symmetry about planes perpendicular to the z- axis, application of the usual boundary conditions gives rise to excess equations (4). Of the combinations studied here, the desired conditions were most nearly met by matching all moments for $\ell < 3$ and the normal moments of order 3 (the f_{31} and f_{33}) at the interface along with the use of the P_{10}, P_{11}, P_{31}, and P_{33} in Marshak's boundary conditions.

The angular flux obtained by matching all moments having $m \neq 0$ plus the f_{00} and f_{10} at the interface, along with the use of the P_{11}, P_{31}, P_{32}, and P_{33} in Marshak's boundary conditions gave a good approximation at the outer boundary, but was found lacking at the interface. Even so, the total flux obtained by using these conditions shows a greater depression in the absorber than the flux obtained by using the preferred boundary conditions, and may more nearly approximate the total flux as described by the exact solution of the Boltzmann equation.

The equivalent radii obtained by fitting the theoretical curve to the experimental data were in error because of the neglect of correction factors, the use of inaccurate cross sections, and uncertainty in the "cleanness" of the counted activity. In spite of these errors the results indicate that with a good experimental determination of the flux and with the correct cross sections, a good determination of the equivalent radius is possible.

3.5 Suggestions for Further Study

Much of the experimental work in the determination of an equivalent rod radius is still to be done. In addition to correcting the faults of the experimental method used in this work, a study of the effect of changes in both scattering and absorption cross sections on the equivalent radius should be made. This analysis could be made rather easily with slight modifications of the computer program described in Appendix D, and it would show which cross sections should be known with the most accuracy. It appears, for example, that the exact value of the moderator absorption cross section is unimportant as long as it is small compared to the scattering cross section.

Since the higher harmonics die out with increasing distance from the source, there should be a region where the total flux is described almost entirely by the first harmonic. By making parallel measurements along the axis of the rod, one should be able to determine whether or not the contribution of the higher harmonics is significant. If the flux can be adequately described by the first harmonic, a considerable amount of computer time can be saved.

If the total flux can be described with the use of only the first harmonic, there is a possibility that the z-dependent model can be replaced by an equivalent unit cell model. The requirement at the cell boundary is that the f_{11}, f_{31}, and f_{33} be zero. An estimate of an appropriate cell boundary could be obtained by plotting the f_{11}, f_{31}, and f_{33} from the z-dependent model and

determining the position at which this requirement is most nearly satisfied. If the unit cell model can be used, the determination of the equivalent rod radius would be greatly simplified.

Although the boundary conditions used in this work give a good approximation to the desired conditions, one further possible combination might be considered. Case 4 was treated rather inconsistently in that some of the moments which were used at the outer boundary were neglected at the interface. Since Case 4 did give a good approximation at the outer boundary, better results might be obtained by neglecting the f_{10} and f_{30} at the interface as well as at the free surface.

ACKNOWLEDGEMENT

The author wishes to express his graditude to Dr. F. S. Prohammer of Argonne National Laboratory, whose original thinking on the subject prompted this study, and to Dr. W. R. Kimel, both for his advice and encouragement, and for bringing this problem to the author's attention. Sincerest thanks are extended to Dr. J. O. Mingle for his advice and encouragement throughout the course of this study, and to W. W. Porath for his wonderful cooperation and effort during the difficult phases of this work. Sincere appreciation is given to W. J. Sturm and the entire staff of the Argonaut Reactor, as well as to the Kansas State University Experiment Station, and the Atomic Energy Commission for their financial support.

LITERATURE CITED

1. Bartels, W. J. C.
   Self-Absorption of Monoenergetic Neutrons. KAPL-336 (1950).

2. Case, K. M., F. de Hoffman, and G. Placzek
   Introduction to The Theory of Neutron Diffusion. Vol. I
   U. S. Govt. Printing Office, Washington D. C., 1953.

3. Davison, B.
   Multilayer Problems in the Spherical Harmonics Method.
   Can. J. Phys. 35,55, 1957.

4. Davison, B. and J. B. Sykes
   Neutron Transport Theory. London: Oxford University, 1958.

5. Faires, R. A. and B. H. Parks
   Radioisotope Laboratory Techniques. New York: Pitman, 1960.

6. Feurzeig, W. and B. I. Spinrad
   Numerical Solution of Transport Theory Problems for Spheres
   and Cylinders. ANL-5049 (1953).

7. Foulke, L. R.
   K.S.U. Pile Standardization and Study of Slowing Down and
   Diffusion Models. M.S. Thesis. Kansas State University,
   1961.

8. Galanin, A. D.
   Thermal Reactor Theory. New York: Pergamon, 1960.

9. Glasstone, S. and E. C. Edlund
   The Elements of Nuclear Reactor Theory.
   Princeton: Van Nostrand, 1952.

10. Hildebrand, F. B.
    Introduction to Numerical Analysis.
    New York: McGraw-Hill, 1956.

11. Jahnke, Emde, and Lösch
    Tables of Higher Functions. New York: McGraw-Hill, 1960.

12. Kofink, W.
    Complete Spherical Harmonics Solution of the Boltzmann
    Equation for Neutron Transport in Homogeneous Media with
    Cylindrical Geometry. Nuc. Sci. and Eng. 6,6, 1959.

13. Lennox, D. H. and C. N. Kelber
    Summary Report on the Hazards of the Argonaut Reactor.
    ANL-5647 (1956).

14. Meghreblian, R. V. and D. K. Holmes
Reactor Analysis. New York: McGraw-Hill, 1960.

15. Porath, W. W.
Unpublished work and private communication. Kansas State University, 1962.

16. Reactor Physics Constants. ANL-5800 (1958).

17. Seren, L
Private communication. Argonne National Laboratory, Argonne, Illinois. Aug. 2, 1962.

18. Stuart, G. W.
A Chart of Neutron Blackness for Solid Cylindrical Rods. HW-34187 (1954).

19. Stuart, G. W.
Neutron Multiple Scattering Methods. A/Conf. 15/P/624 Geneva: United Nations, 1958.

20. Sturm, W. J.
Private communication. Argonne National Laboratory, Argonne, Illinois. Aug. 2, 1962.

21. Sturm, W. J. and D. A. Daavettila
Argonaut Reactor Databook. ANL-6285 (1961).

22. Scarborough, J. B.
Numerical Mathematical Analysis.
Baltimore: John Hopkins, 1950.

23. Tralli, N. and J. Agresta
Spherical Harmonic Corrections for a Cylindrical Cell of Finite Height. Nuc. Sci. and Eng. 10:2, 1961.

24. Weinberg, A. M. and E. P. Wigner
The Physical Theory of Neutron Chain Reactors.
Chicago: University of Chicago, 1958.

25. Wylie, C. R.
Advanced Engineering Mathematics.
New York: McGraw-Hill, 1960.

26. Zink, J. W. and G. W. Rodeback
The Determination of Lattice Parameters by Means of Measurements on a Single Fuel Element. Nuc. Sci. and Eng. 9,16, 1961.

APPENDICES

APPENDIX A

Solution of the P_3 Approximation to the Boltzmann Equation for a Z-Dependent Problem and for the Unit Cell Problem

The spherical harmonics component form of the Boltzmann equation for monoenergetic neutrons at steady state in a homogeneous, isotropic media, for cylindrical geometry, using the $P_{\ell m}(\Omega)$ and nomenclature of Kofink (12), is:

$$\begin{aligned} &A_{\ell m}\left[\frac{\partial}{\partial r}+\frac{m+1}{r}\right]f_{\ell+1}^{m+1}(r,z) - B_{\ell m}\left[\frac{\partial}{\partial r}-\frac{m-1}{r}\right]f_{\ell+1}^{m-1}(r,z) - C_{\ell m}\left[\frac{\partial}{\partial r}+\frac{m+1}{r}\right]f_{\ell-1}^{m+1}(r,z) \\ &+ D_{\ell m}\left[\frac{\partial}{\partial r}-\frac{m-1}{r}\right]f_{\ell-1}^{m-1}(r,z) - E_{\ell m}\frac{\partial}{\partial z}f_{\ell+1}^{m}(r,z) - F_{\ell m}\frac{\partial}{\partial z}f_{\ell-1}^{m}(r,z) \\ &-\left(\Sigma-\frac{4\pi\sigma_{s_\ell}}{2\ell+1}\right)f_{\ell m}(r,z) + Q_{\ell m}(r,z) = 0 \end{aligned} \tag{A-1}$$

where

$$\begin{aligned} A_{\ell m} &= \frac{[(\ell+m+1)(\ell+m+2)]^{1/2}}{2(2\ell+3)} & B_{\ell m} &= \frac{[(\ell-m+1)(\ell-m+2)]^{1/2}}{2(2\ell+3)} \\ C_{\ell m} &= \frac{[(\ell-m-1)(\ell-m)]^{1/2}}{2(2\ell-1)} & D_{\ell m} &= \frac{[(\ell+m-1)(\ell+m)]^{1/2}}{2(2\ell-1)} \\ E_{\ell m} &= \frac{[(\ell+m+1)(\ell-m+1)]^{1/2}}{2\ell+3} & F_{\ell m} &= \frac{[(\ell+m)(\ell-m)]^{1/2}}{2\ell-1} \end{aligned} \tag{A-2}$$

For the z-dependent case it was assumed that $Q_{\ell m} = 0$ and that the neutron sources are in the z = 0 plane. Noting the following relations for the modified Bessel functions of integer order m (25).

$$\begin{aligned} \left[\frac{\partial}{\partial r}+\frac{m+1}{r}\right]I_{m+1}(\alpha r) &= \left[\frac{\partial}{\partial r}-\frac{m-1}{r}\right]I_{m-1}(\alpha r) = \alpha I_m(\alpha r) \\ \left[\frac{\partial}{\partial r}+\frac{m+1}{r}\right]K_{m+1}(\alpha r) &= \left[\frac{\partial}{\partial r}-\frac{m-1}{r}\right]K_{m-1}(\alpha r) = -\alpha K_m(\alpha r) \end{aligned} \tag{A-3}$$

it is seen that a solution of the form

$$\begin{aligned} f_{\ell m}(r,z) = {} & C_1 R_{\ell m}(\alpha) I_m(\alpha r) e^{-\lambda z} + C_2 S_{\ell m}(\alpha) K_m(\alpha r) e^{-\lambda z} \\ & + C_3 T_{\ell m}(\alpha) I_m(\alpha r) e^{\lambda z} + C_4 U_{\ell m}(\alpha) K_m(\alpha r) e^{\lambda z} \end{aligned} \tag{A-4}$$

may satisfy the homogeneous part of Eq.(A-1).

Setting $Q_{\ell m}$ equal to zero, placing Eq.(A-4) into Eq.(A-1),

defining

$$\gamma_\ell = 1 - \frac{4\pi s_\ell}{(2\ell+1)\Sigma} \qquad \text{(A-5)}$$

and equating coefficients of like terms yields the following relations.

$$\begin{aligned}
&\alpha\left(A_{\ell m} R^{m+1}_{\ell+1} - B_{\ell m} R^{m-1}_{\ell+1} - C_{\ell m} R^{m+1}_{\ell-1} + D_{\ell m} R^{m-1}_{\ell-1}\right) + \lambda\left(E_{\ell m} R^{m}_{\ell+1} + F_{\ell m} R^{m}_{\ell-1}\right) = \gamma_\ell R_{\ell m} \\
&-\alpha\left(A_{\ell m} S^{m+1}_{\ell+1} - B_{\ell m} S^{m-1}_{\ell+1} - C_{\ell m} S^{m+1}_{\ell-1} + D_{\ell m} S^{m-1}_{\ell-1}\right) + \lambda\left(E_{\ell m} S^{m}_{\ell+1} + F_{\ell m} S^{m}_{\ell-1}\right) = \gamma_\ell S_{\ell m} \\
&\alpha\left(A_{\ell m} T^{m+1}_{\ell+1} - B_{\ell m} T^{m-1}_{\ell+1} - C_{\ell m} T^{m+1}_{\ell-1} + D_{\ell m} T^{m-1}_{\ell-1}\right) - \lambda\left(E_{\ell m} T^{m}_{\ell+1} + F_{\ell m} T^{m}_{\ell-1}\right) = \gamma_\ell T_{\ell m} \\
&-\alpha\left(A_{\ell m} U^{m+1}_{\ell+1} - B_{\ell m} U^{m-1}_{\ell+1} - C_{\ell m} U^{m+1}_{\ell-1} + D_{\ell m} U^{m-1}_{\ell-1}\right) - \lambda\left(E_{\ell m} U^{m}_{\ell+1} + F_{\ell m} U^{m}_{\ell-1}\right) = \gamma_\ell U_{\ell m}
\end{aligned} \qquad \text{(A-6)}$$

Comparison of the above relations shows that

$$S_{\ell m} = (-1)^m R_{\ell m} \qquad T_{\ell m} = (-1)^{\ell+m} R_{\ell m} \qquad U_{\ell m} = (-1)^\ell R_{\ell m} \qquad \text{(A-7)}$$

Therefore, only the relations for the $R_{\ell m}(\alpha)$ are studied.

If there is no net flow of neutrons around the axis of the cylinder, the condition of symmetry to be satisfied is

$$f(r, z, \theta, \phi) = f(r, z, \theta, -\phi) \qquad \text{(A-8)}$$

This means that only such combinations of $f_{\ell m}(r,z)P_{\ell m}(\underline{\Omega})$ as contain $\cos(m\phi)$ need be retained. For any $m \neq 0$, the angular flux contains pairs of the form

$$(-1)^m f_{\ell,-m}(\cos m\phi - i \sin m\phi) + f_{\ell,m}(\cos m\phi + i \sin m\phi) \qquad \text{(A-9)}$$

By requiring $f_{\ell,-m} = (-1)^m f_{\ell,m}$, the symmetry condition is satisfied. This also requires that

$$R_{\ell,-m} = (-1)^m R_{\ell,m} \qquad \text{(A-10)}$$

Using the above restrictions for the P_3 approximation to the Boltzmann equation ($R_{\ell m} = 0$ for $\ell > 3$), and assuming linear anisotropic scattering ($s_\ell = 0$ for $\ell > 2$), the following set of equations were obtained from the relations for the $R_{\ell m}(\alpha)$ in Eq.(A-6).

$$
\begin{bmatrix}
1 & 0 & 0 & 0 & -\frac{\alpha}{10}\sqrt{30} & 0 & 0 & 0 & 0 & 0 \\
0 & 1 & 0 & 0 & -\frac{\lambda}{\sqrt{5}} & -\frac{\alpha}{\sqrt{5}} & 0 & 0 & 0 & 0 \\
0 & 0 & 1 & 0 & \frac{\alpha}{10}\sqrt{2} & -\frac{2\lambda}{5}\sqrt{2} & -\frac{\alpha}{5}\sqrt{3} & 0 & 0 & 0 \\
0 & 0 & 0 & 1 & 0 & \frac{\alpha}{5}\sqrt{6} & -\frac{3\lambda}{5} & 0 & 0 & 0 \\
-\frac{\alpha}{14}\sqrt{30} & -\frac{\lambda}{7}\sqrt{5} & \frac{\alpha}{14}\sqrt{2} & 0 & 1 & 0 & 0 & -\frac{\alpha}{\sqrt{3}} & 0 & 0 \\
0 & -\frac{\alpha}{7}\sqrt{5} & -\frac{2\lambda}{7}\sqrt{2} & \frac{\alpha}{14}\sqrt{6} & 0 & 1 & 0 & -\frac{\lambda}{\sqrt{3}} & -\frac{\alpha}{\sqrt{2}} & 0 \\
0 & 0 & -\frac{2\alpha}{7}\sqrt{3} & -\frac{3\lambda}{7} & 0 & 0 & 1 & \frac{\alpha}{3}\sqrt{2} & -\frac{2\lambda}{3} & 0 \\
0 & 0 & 0 & 0 & -\frac{\alpha}{5}\sqrt{3} & -\frac{\lambda}{5}\sqrt{3} & \frac{\alpha}{10}\sqrt{2} & \frac{1}{4} & 0 & -\frac{\alpha}{\sqrt{2}} \\
0 & 0 & 0 & 0 & 0 & -\frac{\alpha}{5}\sqrt{6} & -\frac{2\lambda}{5} & 0 & \frac{1}{4} & -\lambda \\
0 & 0 & 0 & 0 & 0 & 0 & 0 & -\frac{\alpha}{3}\sqrt{2} & -\frac{\lambda}{3} & \frac{1}{10}
\end{bmatrix}
\begin{bmatrix} R_{33} \\ R_{32} \\ R_{31} \\ R_{30} \\ R_{22} \\ R_{21} \\ R_{20} \\ R_{11} \\ R_{10} \\ R_{00} \end{bmatrix}
\quad (A\text{-}11) \quad = 0
$$

Using a Crout-type reduction, the above matrix was arranged so that the first four rows were the same as above, the first four columns of rows 5 through 10 contained zeros, and the remainder of the matrix was as shown below.

$$
\begin{bmatrix}
\cdots & \cdots & \cdots \\
\cdots & \cdots & \cdots \\
\cdots & \cdots & \cdots \\
\cdots 1\ 0\ 0\ 0 & \lambda E/A\sqrt{6} & D\sqrt{6}/2A \\
\cdots 0\ \alpha\ 0\ 0 & (\alpha^2-\lambda^2)E/A\sqrt{6} & -\sqrt{6}\,\lambda(\alpha^2+D)/2A \\
\cdots 0\ 0\ A\ 0 & \lambda E & D-2\lambda^2 \\
\cdots 0\ 0\ 0\ 0 & 0 & C \\
\cdots 0\ 0\ 0\ 0 & B & -\lambda(8\alpha^2+9\lambda^2+D-35) \\
\cdots 0\ 0\ 0\ -\alpha\sqrt{2} & -\lambda & 3\frac{1}{10}
\end{bmatrix}
\begin{bmatrix} \cdot \\ \cdot \\ \cdot \\ R_{22} \\ R_{21} \\ R_{20} \\ R_{11} \\ R_{10} \\ R_{00} \end{bmatrix}
\quad (A\text{-}12) \quad = 0
$$

where

$$A = \alpha^2 + \lambda^2 - 7 \qquad D = \alpha^2 - 3\gamma_0\gamma_1 - 7\gamma_0 \qquad E = 3\gamma_1 + 7 \tag{A-13}$$

$$B = (8\gamma_1 + 7)(\alpha^2 + \lambda^2) - 35\gamma_1 \tag{A-14}$$

$$C = 9(\alpha^2 + \lambda^2)^2 - (35 + 27\gamma_0\gamma_1 + 28\gamma_0)(\alpha^2 + \lambda^2) + 105\gamma_0\gamma_1 \tag{A-15}$$

Applying Cramer"s Rule, and setting the determinant of the matrix equal to zero, the characteristic equation is

$$ABC = 0 \tag{A-16}$$

Designating the roots of this equation in the following manner,

$$\begin{aligned} \lambda^2 + \alpha_1^2 &= \tfrac{35}{18}\,\mathcal{G}\left[1 - (1 - 108\gamma_0\gamma_1/35\mathcal{G}^2)^{1/2}\right] = a_1 \\ \lambda^2 + \alpha_2^2 &= \tfrac{35}{18}\,\mathcal{G}\left[1 + (1 - 108\gamma_0\gamma_1/35\mathcal{G}^2)^{1/2}\right] = a_2 \\ \lambda^2 + \alpha_3^2 &= 7 \\ \lambda^2 + \alpha_4^2 &= 35\gamma_1/(8\gamma_1 + 7) = a_4 \end{aligned} \tag{A-17}$$

where

$$\mathcal{G} = 1 + \gamma_0\left(\tfrac{4}{5} + \tfrac{27}{35}\gamma_1\right) \tag{A-18}$$

the general solution for the moments is

$$\begin{aligned} f_{\ell m}(r,z) = \sum_{i=1}^{4} R_{\ell m}(\alpha_i) \Big\{ &\left[C_1 I_m(\alpha_i \Sigma r) + (-1)^m C_2 K_m(\alpha_i \Sigma r)\right] e^{-\lambda \Sigma z} \\ &+ (-1)^\ell \left[C_3 (-1)^m I_m(\alpha_i \Sigma r) + C_4 K_m(\alpha_i \Sigma r)\right] e^{\lambda \Sigma z} \Big\} \end{aligned} \tag{A-19}$$

The $R_{\ell m}$, as given in Table A-1, were obtained by separately placing the roots into the matrix and arbitrarily setting one of the $R_{\ell m}$ equal to 1.

For a medium as shown in Fig. A-1, the cylinder is unbounded in the positive z- direction and the boundary conditions are

$$\lim_{z \to +\infty} f_{\ell m}(r,z) = 0 \qquad \text{(all r)} \tag{A-20}$$

$$f_{\ell m}(0,z) \text{ is finite} \tag{A-21}$$

In addition, the moderator α_1 will be imaginary. Designating the roots of the characteristic equation for the moderator by b_1 and using β_i instead of α_i, the b_1, β_i, and $R_{\ell m}(\beta_i)$ for

Table A-1

Elements of Solution Vectors
for the Z-Dependent Case*

ℓ	m	$R_{\ell m}(\alpha_j)$ $j = 1,2$	$R_{\ell m}(\alpha_3)$	$R_{\ell m}(\alpha_4)$
0	0	1	0	0
1	0	$3\gamma_0\lambda/a_j$	0	1
1	1	$3\gamma_0\alpha_j/a_j\sqrt{2}$	0	$-\lambda/\alpha_4\sqrt{2}$
2	0	$(3\lambda^2-a_j)N_j$	1	$5\gamma_1\lambda/a_4$
2	1	$\alpha_j\lambda N_j\sqrt{6}$	$-2\lambda/\alpha_3\sqrt{6}$	$-5(2\lambda^2-a_4)M/\sqrt{6}$
2	2	$\alpha_j^2 N_j\sqrt{6}/2$	$(\lambda^2+7)/\alpha_3^2\sqrt{6}$	$-5\gamma_1\lambda/a_4\sqrt{6}$
3	0	$3\lambda(5\lambda^2-3a_j)N_j/5$	λ	$\gamma_1(5\lambda^2-a_4)/a_4$
3	1	$3\sqrt{3}\,\alpha_j(5\lambda^2-a_j)N_j/10$	$-(3\lambda^2-7)/2\alpha_3\sqrt{3}$	$-\lambda(15\lambda^2-11a_4)M/2\sqrt{3}$
3	2	$9\lambda\alpha_j^2 N_j/\sqrt{30}$	$\lambda(3\lambda^2-7)/\alpha_3^2\sqrt{30}$	$-5\gamma_1(3\lambda^2-a_4)/a_4\sqrt{30}$
3	3	$3\alpha_j^3 N_j/2\sqrt{5}$	$(\lambda^2+7)/2\alpha_3\sqrt{5}$	$-\sqrt{5}\,\gamma_1\alpha_4\lambda/2a_4$
		$a_j N_j = (a_j-3\gamma_0\gamma_1-7\gamma_0)/(a_j-7)$		$M = \gamma_1/a_4\alpha_4$

*The $R_{\ell m}(\beta_1)$ are obtained from the $R_{\ell m}(\alpha_1)$ by using moderator values of γ_0 and γ_1, replacing a_1 with b_1, replacing α_1 by β_1 and then multiplying by $(-1)^m$.

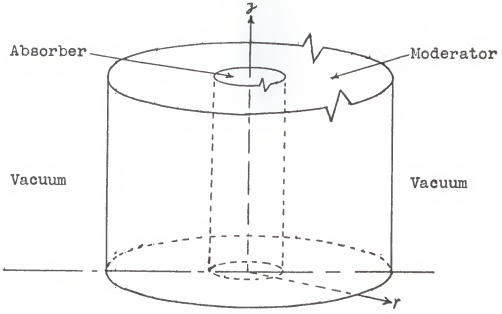

Fig. A-1 Geometry for the Z-Dependent Case

$i \neq 1$ are calculated in the same manner as the corresponding relations in the absorber. For $i = 1$ the $R_{\rho m}(\beta_i)$ are given in Table A-1 and β_1 is given by

$$\lambda^2 - \beta_1^2 = \frac{35}{18} g \left[1 - (1 - 108\,\gamma_0/\gamma_1/35 g^2)^{1/2}\right] = b_1 \qquad \text{(A-22)}$$

Then, the moments for this geometry become, for the absorber (central region)

$$f_{\rho m}(r, z) = \sum_{\alpha=1}^{4} A_\alpha R_{\rho m}(\alpha_\alpha) I_m(\alpha_\alpha \Sigma r)\, e^{-\lambda \Sigma z} \qquad \text{(A-23)}$$

while for the moderator (surrounding medium)

$$f_{\rho m}(r, z) = R_{\rho m}(\beta_1)\left[B_1 J_m(\beta_1 \Sigma r) + C_1 Y_m(\beta_1 \Sigma r)\right] e^{-\lambda \Sigma z} + \sum_{\alpha=2}^{4} R_{\rho m}(\beta_\alpha)\left[B_\alpha I_m(\beta_\alpha \Sigma r) + (-1)^m C_\alpha K_m(\beta_\alpha \Sigma r)\right] e^{-\lambda \Sigma z} \qquad \text{(A-24)}$$

Solution for the Unit Cell Model with Isotropic Source Term

In the unit cell model it is assumed that the z-dependence of the angular flux can be neglected, and that the symmetry condition given by Eq.(A-10) applies. It is also assumed that the slowing down density is zero in the fuel and constant in the moderator. Thus, the equations are homogeneous in the fuel only.

For the equations in the absorber and for the homogeneous part of the equations in the moderator Eq.(A-4) and Eq.(A-6) will apply with $\lambda = 0$. It is seen from Eq.(A-11) that with $\lambda = 0$ the $R_{\ell m}(\alpha)$ having $\ell + m$ odd are completely independent of the $R_{\ell m}(\alpha)$ with $\ell + m$ even. However, the angular flux should be symmetric about any plane perpendicular to the z- axis. This requires that

$$f(r, \theta, \phi) = f(r, \pi - \theta, \phi) \qquad \text{(A-25)}$$

By retaining only the moments with $\ell + m$ even this condition will be satisfied.

Applying the above modifications to Eq.(A-11), and using Cramer's rule on the resulting matrix yielded the following characteristic values.

$$\begin{aligned} \alpha_1^2 &= \tfrac{35}{18} g \left[1 - (1 - 108\, \Sigma_0 \Sigma_1 / 35 g^2)^{1/2}\right] \\ \alpha_2^2 &= \tfrac{35}{18} g \left[1 + (1 - 108\, \Sigma_0 \Sigma_1 / 35 g^2)^{1/2}\right] \\ \alpha_3^2 &= 7 \end{aligned} \qquad \text{(A-26)}$$

where g is given by Eq.(A-18).

Assuming that there is a constant isotropic source term in the moderator and no neutron source in the absorber, the solution for the unit cell model in the absorber (central region) is

$$f_{\ell m}(r) = \sum_{i=1}^{3} A_i R_{\ell m}(\alpha_i) I_m(\alpha_i \Sigma r) \qquad \text{(A-27)}$$

while in the moderator (surrounding medium)

$$f_{\ell m}(r) = \sum_{i=1}^{3} R_{\ell m}(\alpha_i)\left[\theta_i I_m(\beta_i r) + (-1)^m C_i K_m(\beta_i r)\right] + \frac{q_{\ell m}}{\Sigma_a}\delta_{\ell 0}\delta_{m 0} \qquad \text{(A-28)}$$

where the $R_{\ell m}(\alpha_i)$ are given in Table A-2.

Table A-2

Elements of Solution Vectors
for the Unit Cell Model

ℓ	m	$R_{\ell m}(\alpha_j)$ $j = 1, 2$	$R_{\ell m}(\alpha_3)$
0	0	1	0
1	1	$3\gamma_0/\alpha_j\sqrt{2}$	0
2	0	$5N_j/4$	1
2	2	$-5N_j\sqrt{6}/8$	$1/\sqrt{6}$
3	1	$3\alpha_j N_j\sqrt{3}/8$	$\alpha_3/2\sqrt{3}$
3	3	$-3\alpha_j N_j\sqrt{5}/8$	$\alpha_3/2\sqrt{5}$

$$N_j = 1 - 3\gamma_0\gamma_1/\alpha_j^2$$

APPENDIX B

Experimental Work

In the experiment described here, a steel rod was inserted into the thermal column of a reactor and gold "foils" were used to measure the neutron flux in and near the rod. This experiment was conducted in order to provide experimental data for a test of the computer code described in Appendix D, to illustrate a possible procedure for the determination of an "equivalent rod radius", and to provide a rough comparison between experiment and theory.

The thermal column of the Argonaut Reactor at Argonne National Laboratory, Argonne, Illinois was used for this experiment. Details of the Argonaut Reactor, its thermal column, and the "standard" one-slab loading used here can be found in several references (13,21).

A special arrangement which was first used by L. Seren (17) is shown in Fig. B-1. These special stringers replaced the regular J-10 (central) and J-11 stringers in the Argonaut thermal column. A one inch diameter steel rod, 24-inches in length, was placed near the core end of the stringer in the position provided and the remainder of the one-inch channel was filled with one-inch graphite cylinders. The two-inch channel was filled with 1 and 15/16 -inch graphite cylinders.

The 24-inch steel rod was cut into sections 10, 8, and 6 inches long. Slots $\frac{1}{4}$ inch deep and 1/16 inch wide were cut diametrically into both ends of the 10-inch section. The 6-inch

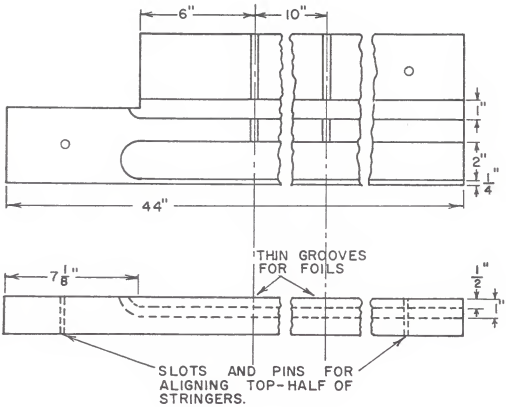

FIG. B-1 SPECIAL J-10 AND J-11 STRINGERS FOR ARGONAUT REACTOR.

section was placed at the core end of the stringer, and the three sections were placed end to end so as to give the appearance of a solid rod having foil slots approximately 6 and 16 inches from the core end of the rod (or approximately 13 and 23 inches from the core end of the J-10 stringer). The Cadmium-ratio at these two points is 15 and 45, respectively (20).

Foils and Counting Facilities

Two types of foils were used to obtain the fine structure near the iron rod. One was a uniform gold wire with a 32-mil diameter. The other was a gold ribbon $\frac{1}{2}$-inch wide by 2-mils thick. Both types of foils were cut into strips approximately $5\frac{1}{2}$-inches long.

The counting system used with the gold wire is shown in Fig. B-2. The shielded end-window G. M. tube was a Nuclear Chicago Model 3031B, serial 344, with U. S. Govt. number 93541. The scaler and power supply were designated by U. S. Govt. number 92121. The central lead shield had originally been designed with a $\frac{1}{4}$ inch diameter opening at the top and with an intersecting wire channel of approximately $\frac{1}{4}$ inch diameter. The central opening was reduced to 1/16 inch by insertion of a small lead plug. The intersecting wire channel was reduced to approximately 1/16 inch by means of plastic tubing.

The gold ribbon was counted in an end window gas flow proportional counter. The counter had U. S. Govt. number 92665, and the scaler and power supply had U. S. Govt. number 92130.

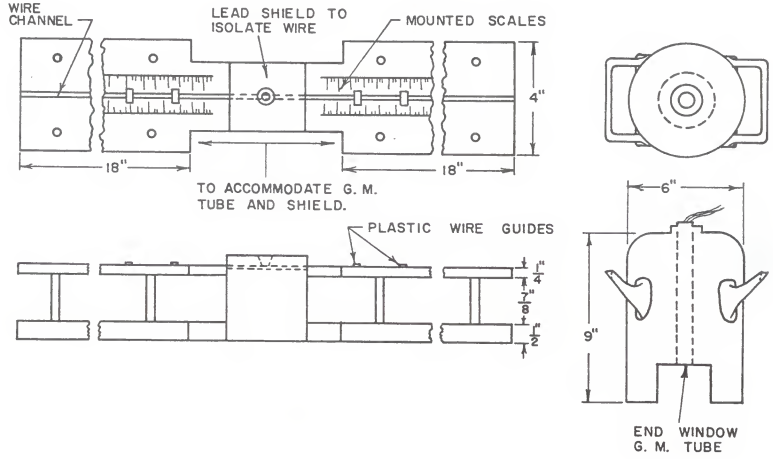

FIG. B-2 WIRE COUNTING EQUIPMENT.

Experimental Procedure

The 5½ inch long foils were placed along the foil grooves and through the steel rod so that one end of the foil was flush with the edge of the J-11 stringer. The reactor was operated at a nominal power of 75 watts for one hour. The stringers were removed with the aid of a threaded rod which screwed into the end of the special stringers. After removal of the foils the iron rod was allowed to "cool" overnight before reusing.

The gold wire was counted in the apparatus shown in Fig. B-2. The wire was visually positioned with the aid of the mounted scales whose smallest division was 1/16 inch. The portion of the wire which had been in or near the rod was counted at 1/16 inch intervals. The remainder of the wire was counted at 1/8 inch intervals. The wire was counted for pre-set times ranging from 2 to 8 minutes, depending on the count rate. The appropriate counting time was chosen so that the standard deviation of the total count at any position was less than 2% of the total count.

The gold ribbon was cut into foils approximately 1/20 of an inch in length by taping the ribbon on graph paper and cutting the ribbon at each division. Every foil which had been in or near the rod was counted and every third foil was counted for the remainder of the region. The foils were counted in the gas flow end window proportional counter for pre-set times. The same criteria was used to determine the counting time as was used for the gold wire. After counting, each foil was weighted on an electric balance.

Treatment of Raw Data

All counts were corrected for background, and those taken with the G. M. tube were corrected for dead time. The dead time correction for the proportional counter was insignificant. The activity was then corrected for decay of the gold nuclei using the well known exponential decay law and a half life of 2.70 days (5). Since only relative activities were of interest, the measured activity at a given position was corrected to the activity present when the first section of the wire or ribbon was counted. The data taken with the gold ribbon was placed on a milligram basis by dividing the activity of each foil by the weight of the foil. All counts obtained from a given $5\frac{1}{2}$-inch gold strip were then placed on the same time basis so that relative count rates at different positions could be compared.

The data processed in the above manner are tabulated in Tables B-1 through B-3. The deviation listed is the standard deviation of the net count rate. In computing the standard deviation for the activity from the gold ribbon it was assumed that the standard deviation in the weights of the foils was 0.025 mg. This figure was arrived at by the following considerations: Since the foil weights could be read accurately to 0.1 mg, the maximum error should be 0.05 mg. If it is assumed that the "maximum" error is of the order of twice the standard deviation, then 0.025 mg is the standard deviation in the weight of a given foil. The combined standard deviation was then calculated in the usual manner (5).

Table B-1

Processed Experimental Data for 1" Rod
Using Gold Wire at Approximately 23"
from Core End of J-10 Stringer

Distance from Rod Center (1/32)-inches	Counts per 4-min	Distance from Rod Center (1/32)-inches	Counts per 4-min
-33	12292 ± 115	21	11114 ± 108
-31	12219 ± 115	23	11755 ± 111
-29	12050 ± 114	25	11938 ± 112
-27	11937 ± 113	27	12039 ± 112
-25	11552 ± 111	29	12158 ± 113
-23	11159 ± 109	31	12164 ± 113
-21	11104 ± 109	33	12327 ± 113
-19	10925 ± 108	37	12741 ± 115
-17	10504 ± 106	41	12775 ± 115
-15	10146 ± 104	45	12808 ± 115
-13	9615 ± 101	49	12916 ± 116
-11	9235 ± 99	53	12983 ± 116
-9	8768 ± 97	57	13033 ± 116
-7	8836 ± 97	59	13406 ± 118
-5	8710 ± 96	61	13235 ± 117
-3	8438 ± 95	63	13004 ± 116
-1	8462 ± 95	65	13190 ± 117
1	8435 ± 95	69	13188 ± 117
3	8387 ± 95	73	13508 ± 118
5	8613 ± 96	77	13546 ± 118
7	8783 ± 97	81	13864 ± 119
9	8922 ± 97	85	13661 ± 118
11	9347 ± 99	89	13257 ± 117
13	9744 ± 101	93	13230 ± 116
15	10325 ± 104	97	13174 ± 116
17	10585 ± 106	101	13179 ± 116
19	11046 ± 108	105	13162 ± 116

Table B-2

Processed Experimental Data for 1" Rod
Using Gold Wire at Approximately 13"
from Core End of J-10 Stringer

Distance from Rod Center (1/32)-inches	Counts per 2-min	Distance from Rod Center (1/32)-inches	Counts per 2-min
-34	13478 ± 118	24	12424 ± 113
-32	13173 ± 117	26	12935 ± 115
-30	12886 ± 116	28	12983 ± 115
-28	13021 ± 116	30	13322 ± 117
-26	12844 ± 115	32	13671 ± 118
-24	12438 ± 113	34	13569 ± 118
-22	12379 ± 113	36	13659 ± 118
-20	12038 ± 112	38	13840 ± 119
-18	11753 ± 110	40	13682 ± 118
-16	11350 ± 108	42	13860 ± 119
-14	11107 ± 107	44	13949 ± 119
-12	10860 ± 106	46	13992 ± 119
-10	10695 ± 105	48	13959 ± 119
-8	10246 ± 103	50	14007 ± 119
-6	10036 ± 102	54	14375 ± 121
-4	10063 ± 102	58	14562 ± 122
-2	9982 ± 102	62	14763 ± 122
0	10115 ± 102	66	14941 ± 123
2	10059 ± 102	70	14769 ± 122
4	10001 ± 102	74	14894 ± 123
6	10112 ± 102	78	15081 ± 124
8	10439 ± 104	82	15189 ± 124
10	10637 ± 105	86	14766 ± 122
12	10950 ± 106	90	14617 ± 122
14	11062 ± 107	94	14261 ± 120
16	11593 ± 109	98	14168 ± 120
18	11893 ± 110	102	14061 ± 119
20	12100 ± 111	106	14086 ± 119
22	12358 ± 113		

Table B-3

Processed Experimental Data for 1" Rod
Using Gold Ribbon at Approximately 13"
from Core End of J-10 Stringer

Distance from Rod Center (1/40)-inches	Counts per 2-min per mg	Distance from Rod Center (1/40)-inches	Counts per 2-min per mg
-50	15391 ± 66	8	10017 ± 48
-48	15580 ± 70	10	10093 ± 48
-46	15530 ± 71	12	10293 ± 48
-44	15268 ± 65	14	10996 ± 60
-42	15345 ± 71	16	11552 ± 49
-40	14982 ± 75	18	11947 ± 57
-38	14630 ± 62	20	12471 ± 57
-36	14508 ± 63	22	13269 ± 63
-34	14728 ± 67	24	13660 ± 60
-32	14095 ± 64	30	14318 ± 64
-30	13718 ± 58	36	14796 ± 67
-28	13375 ± 56	42	15032 ± 62
-26	13125 ± 60	48	15178 ± 63
-24	13009 ± 58	54	15374 ± 70
-22	12734 ± 60	60	15738 ± 71
-20	12364 ± 58	66	15797 ± 67
-18	11715 ± 51	72	16105 ± 76
-16	11133 ± 53	78	16307 ± 67
-14	11056 ± 55	84	16261 ± 69
-12	10905 ± 51	90	16217 ± 71
-10	10481 ± 53	96	16024 ± 65
-8	10297 ± 52	102	16604 ± 79
-6	10107 ± 52	108	16145 ± 69
-4	9956 ± 49	114	16652 ± 74
-2	9857 ± 50	120	16622 ± 68
0	9798 ± 48	126	16636 ± 71
2	9678 ± 46	132	16399 ± 65
4	9714 ± 48	138	16707 ± 68
6	9739 ± 50	144	16917 ± 77

Moderator Radius and Cross Sections

In order to use the P_3 approximation to the Boltzmann equation as described in the theory, the absorption and transport, or scattering cross sections in both moderator and absorber, as well as the physical dimensions of both moderator and absorber, must be known. Although the dimensions of the absorber were well known, the dimensions of an equivalent free surface cylindrical moderator to replace the actual thermal column and surrounding shield had to be estimated.

An attempt was made to determine the equivalent moderator radius by making traverse flux measurements in the Argonaut thermal column and fitting the data with a series of orthogonal Bessel functions of the first kind of zero order. As predicted by diffusion theory, the equivalent radius would then be the point where the resulting curve goes to zero.

The use of just the first term of the series yielded an equivalent radius of approximately 30 inches, which is the actual dimension in the direction of the measurements and also in the direction along the length of the 5½ inch fine structure foils. The data was so erratic however, that higher harmonics yielded unbelievable equivalent radii.

Inasmuch as the flux shape in and near the absorber should be a slowly varying function of moderator radius, for large radii, and since the first harmonic yielded a radius close to the actual radius, the equivalent moderator radius was taken as 30.0 inches.

No direct information was available on the thermal column

cross sections, however a measurement was available which shows the exponential decrease of the flux along the length of the thermal column, so the absorption cross section was calculated from the equation obtained from the P_1 approximation

$$\gamma^2 - \left(\frac{\pi}{2a}\right)^2 - \left(\frac{\pi}{2b}\right)^2 = 3\Sigma_a\Sigma_{tr}$$

where $\gamma = -\frac{\partial \ln \phi}{\partial z}$ and z is the direction along the length of the thermal column. The scattering cross section was taken to be 0.285 cm^{-1} at a graphite density of 1.6 g/cm^3 (16), γ was determined by Springer (20) to be 0.0370 cm^{-1}, and a and b were taken to be the actual physical dimensions of 24 and 30 inches. The absorption cross section of the moderator was thus calculated to be 2.53×10^{-4} cm^{-1}.

The scattering cross section of the iron rod was taken as 0.947 cm^{-1} (16). At the time of this analysis the iron absorption cross section was not known, and the value of 0.259 cm^{-1} was assumed (20). It was later found that the actual absorption cross section, as determined by several measurements at Oak Ridge National Laboratory, is 0.229 cm^{-1}.

The total flux should not be a rapidly varying function of the rod absorption cross section and a similar comparison between theory and experiment would be expected if the correct cross section had been used.

APPENDIX C

Description and Explanation of IBM-1620 Computer Program used to Calculate the Angular Flux at the Interface

This program calculates the angular flux distribution at the interface between two media by using the P_3 approximation to the Boltzmann equation for a system having cylindrical geometry and exponential flux dependence in the z-direction. The program was written in FORTRAN.

The angular flux for this approximation is

$$f(r,z,\theta,\phi) = \sum_{\ell=0}^{3} \sum_{m=-\ell}^{\ell} f_{\ell m}(r,z)\, P_{\ell m}(\theta,\phi) \qquad (C\text{-}1)$$

where $f_{\ell,-m} = (-1)^m f_{\ell m}$, and the $f_{\ell m}$ are as follows:

In the fuel (central region),

$$f_{\ell m}(r,z) = \sum_{i=1}^{4} A_i R_{\ell m}(\alpha_i)\, I_m(\alpha_i \Sigma r)\, e^{-\lambda \Sigma z} \qquad (C\text{-}2)$$

In the moderator (surrounding region),

$$f_{\ell m}(r,z) = R_{\ell m}(\beta_1)\left[B_1 J_m(\beta_1 \Sigma r) + C_1 Y_m(\beta_1 \Sigma r)\right] e^{-\lambda \Sigma z} + \sum_{i=2}^{4} R_{\ell m}(\beta_i)\left[B_i I_m(\beta_i \Sigma r) + (-1)^m C_i K_m(\beta_i \Sigma r)\right] e^{-\lambda \Sigma z} \qquad (C\text{-}3)$$

The $R_{\ell m}$, α, and β are given in Appendix A. The A_1, B_1, and C_1 can be determined from two sets of boundary conditions with this program. One set, which is called Case 2, matches all moments except the f_{30} and f_{32} at the interface, and uses the equations obtained by using the P_{10}, P_{11}, P_{31}, and P_{33} in Marshak's boundary conditions at the moderator free surface. The other set, called Case 4, matches all moments except the f_{20} and f_{30} at the interface, and uses the equations obtained by using the P_{11}, P_{31}, P_{32}, and P_{33} in Marshak's boundary conditions.

The unknowns A_1, B_1, C_1, and λ are determined with the use of the matrix equation $TX = 0$, where X is a column matrix containing the A_i, B_i, and C_i, and T is a square matrix containing the coefficients as given by the boundary conditions. The correct value of λ is taken to be the one which makes the magnitude of the determinant of T the smallest. A_1 is arbitrarly set equal to 1.0 and the other x_1 are determined from the first 11 equations. The determinant of T and the x_1 are calculated with the aid of a special subroutine, CRAM(X), which uses 18 digit arithmetic and performs a Crout reduction with an auxiliary matrix using the method described by Hildebrand (10). The value of the determinant is calculated by multiplying together the diagonal elements of the auxiliary matrix.

Special subroutines are used to calculate the values of the zero and first order Bessel functions and the recursion relations are used to calculate all higher order functions except the $J_2(\beta_i r)$ and $J_3(\beta_i r)$ evaluated at the interface. The argument is small in this case and the first two terms of the series expansion are used.

The R_{jm} are stored in the COEF(I,J) matrix, the α_i, and β_i are stored in TERM(J), the a_1 and b_1 of Table A-1 are stored in ROOT(J), and the $N_j(a_1)$ and $N_j(b_1)$ of Table A-1 are stored in CFR(J).

The proper sequence for loading the input data is shown in the source program. The meaning of the symbols is given in Table C-1.

Table C-1

Input Data

Symbol	Explanation
MM38	= 0 (This was used in program testing)
MM12	= 0 When λ unknown = 1 When λ is known from a previous calculation and only angular flux is desired
MM	= 1 For Case 4 boundary conditions = 2 For Case 2 boundary conditions
GAM0(1)	Σ_a/Σ in fuel
GAM0(2)	Σ_a/Σ in moderator
GAM1(1)	Σ_{tr}/Σ in fuel
GAM1(2)	Σ_{tr}/Σ in moderator
SIGF	Σ in fuel (cm^{-1})
RF	Rod radius (cm)
SIGM	Σ in moderator (cm^{-1})
RM	Moderator radius (cm)
CRIT1	Convergence criteria for λ (1.0×10^{-8})
DL	Increment in λ
AL	Trial λ

Most of the output is self explanatory, however all input data is printed out immediately after being read in, and this output is unlabled. The dimensions on all output data is in CGS units. The meaning of all symbols and words used in the output is given in Table C-2.

Approximately one and one-half minutes is required for one calculation of SUM. If the original estimate of λ is reasonably close to the correct value, the interpolation converges after about three trials (approximately 5 minutes). A rough first estimate of λ can be obtained from the P_1 approximation for a one region medium.

Table C-2

Output

Symbol	Explanation
DELTA LAMBDA = 0	(Difference of new λ and old λ is zero, program continues)
R(I+1)	Values are listed in the following order: $A_2, A_3, A_4, C_1, C_2, C_3, C_4, B_1, B_2, B_3, B_4$ (note that $A_1 = 1.0$)
PHI	ϕ (radians)
F	Angular flux
THETA	θ (radians)
SUM	Value of determinant of T
SLOPE	Change in SUM divided by change in λ
LAMBDA	λ
IN FUEL	Angular flux evaluated using f_{fm} of Eq.(C-2)
IN MODERATOR	Angular flux evaluated using f_{fm} of Eq.(C-3)
FLUX INWARD	$\int_{\pi/2}^{3\pi/2}\int_{0}^{\pi} f(r,\gamma,\theta,\phi)\sin\theta\, d\theta\, d\phi$
ANGULAR FLUX AVERAGED OVER THETA	$\int_{0}^{\pi} f(r,\gamma,\theta,\varphi)\sin\theta\, d\theta$

The sense switches do not alter the program when in the off position. The changes which occur when they are in the on position are given in Table C-3.

Table C-3

Sense Switches

Switch	Operation When Switch On
1	Not used
2	Causes SUM, SLOPE, and LAMBDA to be typed after each trial
3	Causes CRAM(X) subroutine to type out T matrix
4	Not used

LOGIC DIAGRAM FOR APPENDIX C

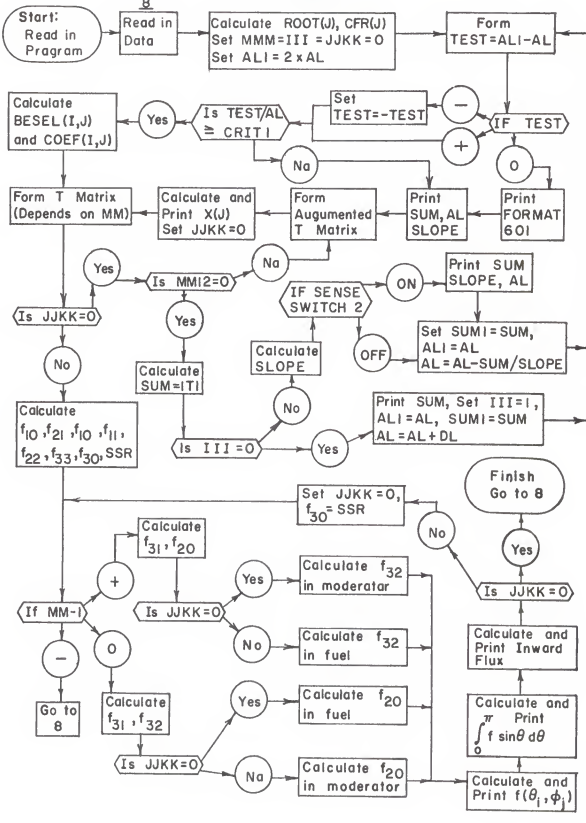

```
C     ITERATES FOR LAMBDA AND CALCULATES ANGULAR DISTRIBUTION
C     AT BOUNDARY, BOTH IN MODERATOR AND IN FUEL
C
      DIMENSION T(12,13),X(12),ROOT(8),TERM(8),ARG(20)
      DIMENSION BESEL(20,4),GAM0(2),GAM1(2),COEF(10,12),CFR(6)
    1 FORMAT(E16.7,E16.7,E16.7,E16.7)
    2 FORMAT(F16.7/)
    3 FORMAT(E16.7,E16.7,E16.7/)
    4 FORMAT(I5,I5,I5,I5,I5,I5)
    5 FORMAT(E16.7,E16.7,E16.7,E16.7,E16.7/)
    6 FORMAT(E16.7,E16.7/)
    7 FORMAT(E14.7,I6,E14.7)
    8 READ 4,MM38,MM12,MM
      TYPE 4,MM38,MM12,MM
      READ 1,GAM0(1),GAM0(2),GAM1(1),GAM1(2)
      TYPE 1,GAM0(1),GAM0(2),GAM1(1),GAM1(2)
      READ 1,SIGF,RF,SIGM,RM
      TYPE 1,SIGF,RF,SIGM,RM
      READ 1,CRIT1,DL,AL
      TYPE 3,CRIT1,DL,AL
      J=1
      K=1
   12 K1=J+1
      A=1. +GAM0(K)*(.8 + 27.*GAM1(K)/35.)
      ROOT(J)= 35.*A*(1.-SQRT(1.-108.*GAM0(K)*GAM1(K)/(35.*A**2)))/18.
      ROOT(J+1)=35.*A*(1.+SQRT(1.-108.*GAM0(K)*GAM1(K)/(35.*A**2)))/18.
      ROOT(J+2)=35.*GAM1(K)/(8.*GAM1(K)+7.)
      ROOT(J+3)=7.
      DO 9 I=J,K1
    9 CFR(I)=(ROOT(I)-GAM0(K)*(3.*GAM1(K)+7.))/(ROOT(I)*(ROOT(I)-7.))
      IF(J-1)8,10,11
   10 J=5
      K=2
      GO TO 12
   11 MMM=0
      JJKK 0
      AL1=2.*AL
      III=0
   80 KKK=0
   90 TEST=AL1-AL
      IF(TEST)91,92,93
   91 TEST=-TEST
   93 IF(TEST/AL-CRIT1)316,94,94
   92 PRINT 601
  601 FORMAT(17H DELTA LAMBDA = 0/)
      GO TO 216
   94 SL=AL**2
  110 DO 111 J=1,8
      IF(J-5)112,111,112
  112 TERM(J)=SQRT(ROOT(J)-SL)
  111 CONTINUE
      TERM(5)=SQRT(SL-ROOT(5))
      DO 113 J=1,4
```

```
      ARG(J)=TERM(J)*SIGF*RF
      ARG(J+4)=TERM(J+4)*SIGM*RF
      ARG(J+8)=ARG(J+4)
      ARG(J+12)=TERM(J+4)*SIGM*RM
113   ARG(J+16)=ARG(J+12)
202   DO 114 J=1,20
      IF(J-5)115,118,119
115   BESEL(J,1)=IZER(ARG(J))
      BESEL(J,2)=IONE(ARG(J))
      A= -1.
124   B= -A
      GO TO 123
118   BESEL(J,1)=YZER(ARG(J))
      BESEL(J,2)=YONE(ARG(J))
      GO TO 120
119   IF(J-9)121,116,122
121   BESEL(J,1)=KZER(ARG(J))
      BESEL(J,2)=KONE(ARG(J))
      A=1.
      B=A
      GO TO 123
116   BESEL(J,1)=JZER(ARG(J))
      BESEL(J,2)=JONE(ARG(J))
      IF(J-9)120,125,120
125   BESEL(J,3)=(ARG(J)**2)*(1.-ARG(J)**2/12.)/8.
      BESEL(J,4)=(ARG(J)**3)*(1.-ARG(J)**2/16.)/48.
      GO TO 114
120   A=1.
      GO TO 124
122   IF(J-13)115,118,117
117   IF(J-17)121,116,115
123   BESEL(J,3)=2.*A*BESEL(J,2)/ARG(J)  +B*BESEL(J,1)
      BESEL(J,4)=4.*A*BESEL(J,3)/ARG(J)  +B*BESEL(J,2)
114   CONTINUE
206   A=-1.
      B=A
      C=-A
      L=1
      M=2
      K=L
133   DO 130 J=L,M
      COEF(1,J)=A
      COEF(2,J)=B*6.*TERM(J)*AL*CFR(J)
      COEF(3,J)=A*3.*GAM0(K)*AL/ROOT(J)
      COEF(4,J)=A*(3.*SL-ROOT(J))*CFR(J)
      COEF(5,J)=C*TERM(J)*COEF(3,J)/AL
      COEF(6,J)=-B*3.*(SL-ROOT(J))*CFR(J)
      COEF(7,J)=3.*AL*COEF(6,J)
      COEF(10,J)=A*3.*AL*(5.*SL-3.*ROOT(J))*CFR(J)/5.
      COEF(8,J)=C*TERM(J)*COEF(6,J)/2.
130   COEF(9,J)=B*9.*TERM(J)*(5.*SL-ROOT(J))*CFR(J)/10.
      IF(M-2)132,132,131
132   L=5
```

```
      K=2
      A=-A
  136 C=-C
      M=L
      GO TO 133
  131 IF(M-5)135,135,134
  135 L=6
      B=-B
      GO TO 136
  134 K=1
      A=-1.
      J=3
  142 COEF(1,J)=0.
      COEF(2,J)=-A*5.*GAM1(K)*(2.*SL-ROOT(J))/(TERM(J)*ROOT(J))
      COEF(3,J)=A
      COEF(4,J)=A*5.*GAM1(K)*AL/ROOT(J)
      COEF(5,J)=-A*AL/TERM(J)
      COEF(6,J)=-COEF(4,J)
      COEF(7,J)=-A*5.*GAM1(K)*(3.*SL-ROOT(J))/ROOT(J)
      COEF(8,J)=-TERM(J)*COEF(4,J)/2.
      COEF(9,J)=-A*GAM1(K)*AL*(15.*SL-11.*ROOT(J))/(2.*ROOT(J)*TERM(J))
      COEF(10,J)=A*GAM1(K)*(5.*SL-ROOT(J))/ROOT(J)
      COEF(1,J+1)=0.0
      COEF(2,J+1)=-A*2.*AL/TERM(J+1)
      COEF(3,J+1)=0.0
      COEF(4,J+1)=A
      COEF(5,J+1)=0.0
      COEF(6,J+1)=-A*(SL+ROOT(J+1))/(SL-ROOT(J+1))
      COEF(7,J+1)=-A*AL*(3.*SL-ROOT(J+1))/(SL-ROOT(J+1))
      COEF(8,J+1)=-A*(SL+ROOT(J+1))/(2.*TERM(J+1))
      COEF(9,J+1)=-A*(3.*SL-ROOT(J+1))/(2.*TERM(J+1))
      COEF(10,J+1)=-A*AL
      IF(J-3)141,140,141
  140 J=7
      A=-A
      K=2
      GO TO 142
  141 DO 146 K=5,8
      DO 147 J=1,10
  147 COEF(J,K+4)=COEF(J,K)
      IF(K-5)146,146,148
  148 DO 149 J=2,8,3
  149 COEF(J,K)=-COEF(J,K)
      COEF(9,K)=-COEF(9,K)
  146 CONTINUE
  211 DO 150 J=1,12
      DO 151 K=1,3,2
  151 T(K,J)=COEF(K,J)*BESEL(J,1)
      IF(MM-1)713,714,713
  714 T(4,J)=COEF(9,J)*BESEL(J,2)
      GO TO 715
  713 T(4,J)=COEF(4,J)*BESEL(J,1)
  715 DO 152 K=2,5,3
```

```
  152 T(K,J)=COEF(K,J)*BESEL(J,2)
      T(6,J)=COEF(6,J)*BESEL(J,3)
      IF(MM-1)730,730,731
  730 T(7,J)=COEF(7,J)*BESEL(J,3)
      GO TO 150
  731 T(7,J)=COEF(9,J)*BESEL(J,2)
  150 T(8,J)=COEF(8,J)*BESEL(J,4)
      DO 155 J=9,12
      DO 155 K=1,4
  155 T(J,K)=0.0
      DO 156 J=5,12
      T(9,J) =COEF(1,J)*BESEL(J+8,1) +2.*COEF(5,J)*BESEL(J+8,2)/3.
      T(9,J) = T(9,J)-(COEF(4,J)*BESEL(J+8,1)-COEF(6,J)*BESEL(J+8,3))/8.
      IF(MM-1)720,721,720
  720 T(10,J)=2.*COEF(3,J)*BESEL(J+8,1)/3. +COEF(2,J)*BESEL(J+8,2)/4.
      GO TO 722
  721 T(10,J)=-COEF(6,J)*BESEL(J+8,3)/48. +8.*COEF(9,J)*BESEL(J+8,2)/21.
      T(10,J)=T(10,J) +(COEF(1,J)/4. +7.*COEF(4,J)/16.)*BESEL(J+8,1)
  722 IF(MM-1)723,723,724
  723 T(11,J)=COEF(2,J)*BESEL(J+8,2)/8. +4.*COEF(7,J)*BESEL(J+8,3)/35.
      GO TO 725
  724 T(11,J)=-COEF(6,J)*BESEL(J+8,3)/48. +8.*COEF(9,J)*BESEL(J+8,2)/21.
      T(11,J)=T(11,J) +(COEF(1,J)/4. +7.*COEF(4,J)/16.)*BESEL(J+8,1)
  725 T(12,J)=-COEF(1,J)*BESEL(J+8,1)/4. +8.*COEF(8,J)*BESEL(J+8,4)/35.
      T(12,J)=T(12,J) +COEF(4,J)*BESEL(J+8,1)/16.
  156 T(12,J)=T(12,J) +3.*COEF(6,J)*BESEL(J+8,3)/16.
  160 IF(JJKK)1160,1160,944
 1160 IF(MM12)161,161,352
  161 IF(MM38)902,902,901
  902 SUM=CRAM(-12.)
      GO TO 299
  901 X(1)=CRAM(12.)
      PRINT 610
  610 FORMAT(5X7H R(I+1)/)
      DO 935 J=1,10
  935 PRINT 1,X(J)
      PRINT 2,X(11)
      JJKK=1
      GO TO 211
  944 DO 945 J=1,8
  945 ARG(J)= -T(J,1)
      DO 946 J=1,8
      DO 946 K=1,3
  946 ARG(J)=ARG(J) -X(K)*T(J,K+1)
      F00=ARG(1)
      F21=ARG(2)
      F10=ARG(3)
      F11=ARG(5)
      F22=ARG(6)
      F33=ARG(8)
      SSR=-COEF(10,1)*BESEL(1,1)
      F30=0.
      DO 1618 J=1,3
```

```
1618 SSR=SSR -X(J)*COEF(10,J+1)*BESEL(J+1,1)
     DO 1619 J=4,11
1619 F30=F30 +X(J)*COEF(10,J+1)*BESEL(J+1,1)
1513 IF(MM-1)8,500,501
 500 F31=ARG(4)
     F32=ARG(7)
     IF(JJKK)1500,1500,1501
1501 F20=0.
     DO 1502 J=4,11
1502 F20=F20 +X(J)*COEF(4,J+1)*BESEL(J+1,1)
     GO TO 502
1500 F20= -COEF(4,1)*BESEL(1,1)
     DO 1503 J=1,3
1503 F20=F20 -X(J)*COEF(4,J+1)*BESEL(J+1,1)
     GO TO 502
 501 F31=ARG(7)
     F20=ARG(4)
     IF(JJKK)1521,1521,1522
1522 F32=0.
     DO 1523 J=4,11
1523 F32=F32 +X(J)*COFF(7,J+1)*BESEL(J+1,3)
     GO TO 502
1521 F32= -COEF(7,1)*BESEL(1,3)
     DO 1524 J=1,3
1524 F32=F32 -X(J)*COEF(7,J+1)*BESEL(J+1,3)
 502 IF(JJKK)503,503,504
 504 PRINT 698
 698 FORMAT(20X13H IN MODERATOR/)
     GO TO 505
 503 PRINT 699
 699 FORMAT(20X8H IN FUEL/)
 505 PRINT 622
 622 FORMAT(7X4H PHI,13X2H F,12X6H THETA/)
     THETA=0.
     F=F00 +F10 +F20 +F30
     PRINT 666,F,THETA
 666 FORMAT(3X13H ALL VALUES  ,E16.7,E16.8)
     DO 350 I=1,5
     PHI=0.0
     THETA=THETA+.5235988
     CY=COS(THETA)
     SY=SIN(THETA)
     IF(I-3)351,532,351
 532 CY=0.
 351 DO 350 J=1,11
     CPHI=COS(PHI)
     CPHI2=COS(2.*PHI)
     CPHI3=COS(3.*PHI)
     IF(J-6)371,372,371
 372 CPHI=0.0
     CPHI3=0.0
 371 F=F00 +F10*CY -F11*SY*CPHI +F20*(3.*(CY**2)-1.)/2.
     F=F-F21*SY*CY*CPHI +F22*(SY**2)*CPHI2/2.
```

```
      F=F +F30*(5.*(CY**3)-3.*CY)/2. +F32*(SY**2)*CY*CPHI2/2.
      F=F-F31*SY*(5.*(CY**2)-1.)*CPHI/2. -F33*(SY**3)*CPHI3/2.
      IF(J-1)359,359,358
  359 PRINT 1,PHI,F,THETA
      GO TO 350
  358 PRINT 1,PHI,F
  350 PHI=PHI +.3141593
      THETA=3.1415927
      F= F00 -F10 +F20 -F30
      PRINT 666,F,THETA
      PRINT 631
  631 FORMAT(7X4H PHI,3X33H ANGULAR FLUX AVERAGED OVER THETA/)
      PI = 3.1415927
      PHI = 0.0
      DO 766 I =1,11
      CPHI=COS(PHI)
      CPHI2=COS(2.*PHI)
      CPHI3=COS(3.*PHI)
      IF(I-6) 382,381,382
  381 CPHI=0.0
      CPHI3=0.0
  382 FA=2.*F00 -PI*F11*CPHI/2. +2.*F22*CPHI2/3.
      FA=FA-PI*F31*CPHI/16. -PI*3.*CPHI3*F33/16.
      PRINT 1,PHI,FA
  766 PHI = PHI +.3141593
      FIN=PI*(2.*F00 +F11 +F31/8. -F33/8.)
      PRINT 638,FIN
  638 FORMAT(E16.7,14H = FLUX INWARD/)
      IF(JJKK)8,8,1512
 1512 JJKK=0
      F30=SSR
      GO TO 1513
  299 IF(III)300,300,304
  300 III=1
      PRINT 602, SUM
  602 FORMAT(E16.7,6H = SUM/)
      AL1=AL
      SUM1=SUM
      AL=AL+DL
      GO TO 90
  304 SLOPE=(SUM-SUM1)/(AL-AL1)
      IF(SENSE SWITCH 2)330,313
  330 IF(KKK)314,314,315
  314 KKK=1
      PRINT 604
  315 PRINT 3,SUM,SLOPE,AL
  313 SUM1=SUM
      AL1=AL
      AL=AL-SUM/SLOPE
      GO TO 90
  316 PRINT 604
  604 FORMAT(8X4H SUM,9X6H SLOPE,11X7H LAMBDA/)
      PRINT 3,SUM,SLOPE,AL1
```

```
352 DO 317 J=1,12
317 T(J,13)= -T(J,1)
    DO 318 J=1,11
    DO 318 I=1,11
318 T(J,I)=T(J,I+1)
    DO 319 J=1,11
    T(J,12)=0.
319 T(12,J)=0.
    MM38=1
    GO TO 161
    END
```

APPENDIX D

Description and Explanation of IBM-1620 Computer Program used to Determine an Equivalent Radius

This program uses an interpolation procedure to calculate the fuel rod radius which makes the sum of the weighted squares of the residuals between experimental and theoretical values of the total neutron flux a minimum. The program was written in FORTRAN.

The total neutron flux in a two region cylindrical medium is described by the P_3 approximation to the Boltzmann equation for neutron transport. The total flux is proportional to f_{00} and the general $f_{\ell m}$ can be written in the form

$$f_{\ell m}(r,z) = \sum_{i=1}^{\infty} D_i G^i_{\ell m}(r,z) \qquad \text{(D-1)}$$

where in the fuel (central region)

$$G^i_{\ell m}(r,z) = \sum_{n=1}^{4} A^i_n R_{\ell m}(\alpha^i_n) I_m(\alpha^i_n \Sigma r) e^{-\lambda_i \Sigma z} \qquad \text{(D-2)}$$

and in the moderator (surrounding region)

$$G^i_{\ell m}(r,z) = R_{\ell m}(\beta^i_1)\left[B^i_1 J_m(\beta^i_1 \Sigma r) + C^i_1 Y_m(\beta^i_1 \Sigma r)\right] e^{-\lambda_i \Sigma z} + \sum_{n=2}^{4} R_{\ell m}(\beta^i_n)\left[B^i_n I_m(\beta^i_n \Sigma r) + (-1)^m C^i_n K_m(\beta^i_n \Sigma r)\right] e^{-\lambda_i \Sigma z} \qquad \text{(D-3)}$$

The $R_{\ell m}$, ω_n, and β_n are given in Appendix A. The A^i_n, B^i_n, and C^i_n, in terms of $A^i_1 = 1.0$, and the λ_i are calculated numerically in this program by the method described in Appendix C and in the Discussion. For boundary conditions, all $f_{\ell m}$ except f_{30} and f_{32} are matched at the interface, and the equations obtained by using P_{10}, P_{11}, P_{31}, and P_{33} in Marshak's boundary conditions at the moderator free surface are used.

By considering only the radial variation of the flux at the points r_j, and defining

$$F_{ij} = G_{oo}(r_j, z) e^{+\lambda_i z} \qquad \text{(D-4)}$$

the sum of the weighted squares of the residuals can be written as

$$E = \sum_{j=1}^{N} w_j \left[\sum_i D_i F_{ij} - \Phi_j\right]^2 \qquad \text{(D-5)}$$

where w_j is the weighting function and Φ_j is the experimental value of the total flux at the point r_j.

In this program an initial estimate of the rod radius is used to calculate the F_{ij}, the D_i are determined by the least squares procedure, E is calculated, the rod radius is changed, and the process is repeated. After three values of E have been calculated, new values of the rod radius are predicated by a second order polynomial of E as a function of rod radius. This process continues until the change in the rod radius, divided by the rod radius, is less than a specified precision.

The program is arranged so that it may be taken off the computer after any given λ has been determined or after E and a new rod radius have been calculated, without destroying the mechanism which has been set up to predict new values of λ and rod radius. The previous values must be used as input in the succeeding calculation however.

The proper sequence for loading the input data is shown in the source program. The meaning of the symbols is given in Table D-1.

Table D-1

Input Data

Symbol	Explanation
NMOD	Number of data points
MMM	= 0 when no previous value of E is known = 1 when one previous value of E is known = 2 when two previous values of E are known
GAMO(1)	Σ_a/Σ in fuel
GAMO(2)	Σ_a/Σ in moderator
GAM1(1)	Σ_{tr}/Σ in fuel
GAM1(2)	Σ_{tr}/Σ in moderator
SIGF	Σ in fuel (cm^{-1})
SIGM	Σ in moderator (cm^{-1})
RM	Moderator radius (cm)
CRIT1	Convergence criteria for λ (1.0×10^{-8})
CRIT2	Convergence criteria for rod radius
FACTR	Factor used to convert radial position of data points into CGS units
DIV1	Factor used to convert radial position of data points into CGS units
DLTRF	Increment in rod radius
EERR(1)	Next to last value of E if MMM = 2 Last value of E when MMM = 1
EERR(2)	Last value of E when MMM = 2
RRF(1)	Rod radius corresponding to EERR(1)
RRF(2)	Rod radius corresponding to EERR(2)
PHI(J)	Data points in order from center out
K	Any integer
W(J)	Reciprocal of square root of weighting factor, in order from center out
A	Radial position of data points in order of increasing r (any units)
NC	Number of harmonics
RF	Trial rod radius (cm)
ADD1	1.0×10^{-7} (used to increment λ slightly)
DL	Increment in λ
AAL(J)	Trial λ_j in order of increasing j up to j = NC
AALO(J)	λ_j from previous calculation, in order of increasing j
SLOPE(J)	SLOPE(J) from preceding calculation
INDEX(J)	= 0 if λ_j unknown = 1 if λ_j known

All of the output is labled, however some of the input data is printed out immediately after being read in, and this output is unlabled. The dimensions on all labled output is in CGS units. The meaning of all words and symbols used in the output is given in Table D-2.

Table D-2

Output

Symbol	Explanation
DELTA LAMBDA = 0	(Difference of new λ and old λ is zero, program continues)
DELTA RADIUS = 0	(Difference of new rod radius and old rod radius is zero, problem is finished and program goes back to start)
SUM	Value of the determinant of T
SLOPE	Change in SUM divided by change in λ
LAMBDA	λ
R(I+1)	Values are listed in the following order: $A_2, A_3, A_4, C_1, C_2, C_3, C_4, B_1, B_2, B_3, B_4$ (note that $A_1 = 1.0$)
COEFICIENTS	D_i of Eq.(D-1)
CALCULATED FLUX	Total neutron flux at r_i
RADIUS	Radial position of CALCULATED FLUX and of experimental data points
ROD RADIUS	Fuel rod radius
ERROR	E (Least squares error)

If the initial estimate of λ is reasonably close to the correct value, approximately 5 minutes of computer time is required to determine the correct λ and the corresponding x_i for each harmonic used. For 37 data points, approximately 5 additional minutes is required to calculate the error and a new rod radius after λ has been determined. An additional 5 minutes is required for each additional harmonic.

The sense switches do not alter the program when in the off position. The changes which occur when they are in the on position are given in Table D-3.

Table D-3

Sense Switches

Switch	Operation When Switch On
1	Punch R(I+1) Punch RF, CALCULATED FLUX, and RADIUS
2	Print SUM, SLOPE, and LAMBDA after each trial
3	Causes CRAM(X) subroutine to type out T matrix
4	Interpolation for rod radius is bypassed, new values of RF must be read in

LOGIC DIAGRAM FOR APPENDIX D

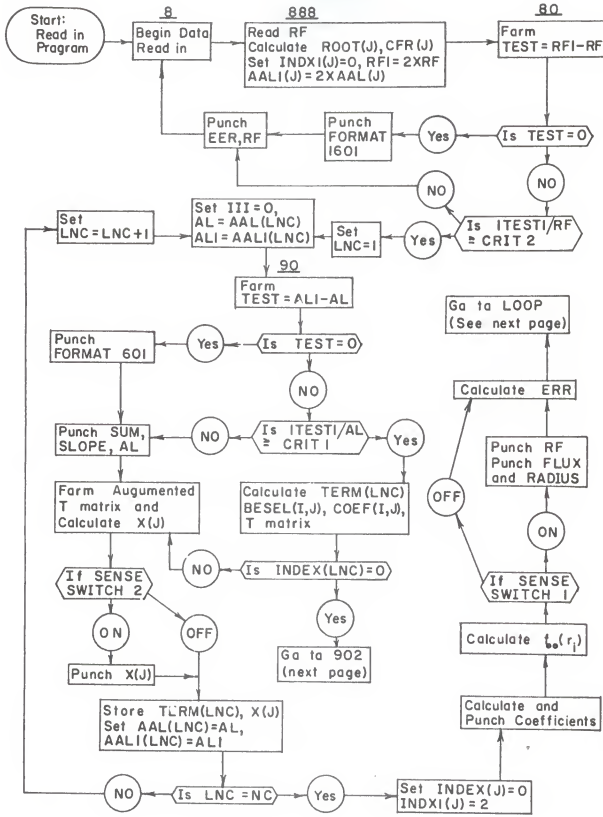

LOGIC DIAGRAM (CONT'D)
APPENDIX D

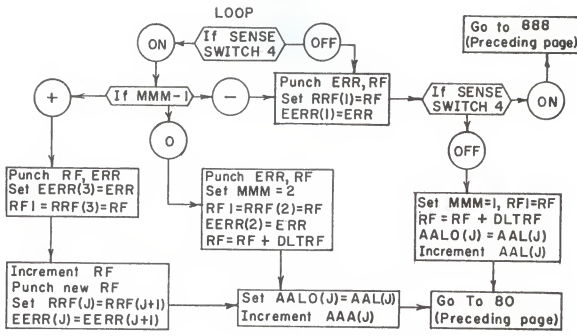

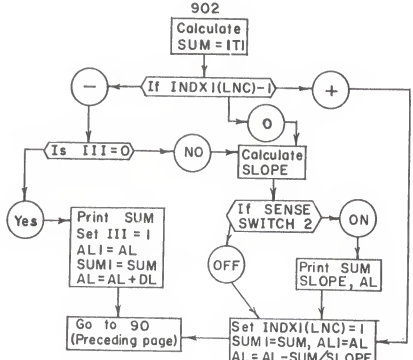

```
C   LEAST SQUARES PROGRAM USING UP TO 4 HARMONICS, P3 APPROXIMATION
C
      DIMENSION T(12,13),X(12),ROOT(8),TERM(8),ARG(20)
      DIMENSION PHI(50),R(50),W(50),ALSIG(4),BTSIG(4),ENSIG(4)
      DIMENSION BESEL(50,4),GAM0(2),GAM1(2),COEF(8,12),CFR(6)
      DIMENSION OMSIG(4),Z(36),TEEM(32),AAL(4),AAL1(4),INDEX(4)
      DIMENSION SLOPE(4),AAL0(4),RRF(3),EERR(3),INDX1(4)
    1 FORMAT(E16.7,E16.7,E16.7,E16.7)
    2 FORMAT(E16.7/)
    3 FORMAT(E16.7,E16.7,E16.7/)
    4 FORMAT(I5,I5,I5,I5,I5,I5)
    5 FORMAT(E16.7,E16.7,E16.7,E16.7/)
    6 FORMAT(E16.7,E16.7/)
    7 FORMAT(E14.7,I6,E14.7)
C
    8 READ 4,NMOD,MMM
      PRINT 4,NMOD,MMM
      PUNCH 4,NMOD,MMM
      READ 1,GAM0(1),GAM0(2),GAM1(1),GAM1(2)
      PUNCH 1,GAM0(1),GAM0(2),GAM1(1),GAM1(2)
      READ 1,SIGF,SIGM,RM,CRIT1
      PUNCH 1,SIGF,SIGM,RM,CRIT1
      READ 1,CRIT2,FACTR,DIV1,DLTRF
      PUNCH 1,CRIT2,FACTR,DIV1,DLTRF
      READ  1,EERR(1),EERR(2),RRF(1),RRF(2)
      PUNCH 1,EERR(1),EERR(2),RRF(1),RRF(2)
      DO 15 J=1,NMOD
      READ 7,PHI(J),K,W(J)
   15 W(J)=1./(W(J)**2)
      DO 16 J=1,NMOD
      READ 1,A
   16 R(J)=A*FACTR/DIV1
      READ 4,NC
      PUNCH 4,NC
  888 READ 1,RF,ADD1,DL
      DO 3115 J=1,NC
      READ 1,AAL(J),AAL0(J),SLOPE(J)
      READ 4,INDEX(J)
      AAL1(J)=2.*AAL(J)
      INDX1(J)=0
 3115 PUNCH 1,AAL(J),AAL0(J),SLOPE(J)
      PRINT 3,RF,ADD1,DL
      PUNCH 3,RF,ADD1,DL
C
      J=1
      K=1
   12 K1=J+1
      A=1. +GAM0(K)*(.8 + 27.*GAM1(K)/35.)
      ROOT(J)= 35.*A*(1.-SQRT(1.-108.*GAM0(K)*GAM1(K)/(35.*A**2)))/18.
      ROOT(J+1)=35.*A*(1.+SQRT(1.-108.*GAM0(K)*GAM1(K)/(35.*A**2)))/18.
      ROOT(J+2)=35.*GAM1(K)/(8.*GAM1(K)+7.)
      ROOT(J+3)=7.
      DO 9 I=J,K1
```

```
    9 CFR(I)=(ROOT(I)-GAM0(K)*(3.*GAM1(K)+7.))/(ROOT(I)*(ROOT(I)-7.))
      IF(J-1)8,10,11
   10 J=5
      K=2
      GO TO 12
   11 RF1=2.*RF
   80 TEST=RF1-RF
      IF(TEST)81,82,83
   81 TEST=-TEST
   83 IF(TEST/RF-CRIT2)1316,900,900
   82 PRINT 1601
 1601 FORMAT(17H DELTA RADIUS = 0/)
      GO TO 1316
C
C     FROM HERE TO 1800 FINDS EIGEN-VALUE AND EIGEN-VECTORS
C
  900 DO 1800 LNC=1,NC
      III=0
      KKK=0
      AL=AAL(LNC)
      AL1=AAL1(LNC)
   90 TEST=AL1-AL
      IF(TEST)91,92,93
   91 TEST=-TEST
   93 IF(TEST/AL-CRIT1)316,94,94
   92 PUNCH 601
  601 FORMAT(17H DELTA LAMBDA = 0/)
      GO TO 316
   94 SL=AL**2
  110 DO 111 J=1,8
      IF(J-5)112,111,112
  112 TERM(J)=SQRT(ROOT(J)-SL)
  111 CONTINUE
      TERM(5)=SQRT(SL-ROOT(5))
      DO 113 J=1,4
      ARG(J)=TERM(J)*SIGF*RF
      ARG(J+4)=TERM(J+4)*SIGM*RF
      ARG(J+8)=ARG(J+4)
      ARG(J+12)=TERM(J+4)*SIGM*RM
  113 ARG(J+16)=ARG(J+12)
      DO 114 J=1,20
      IF(J-5)115,118,119
  115 BESEL(J,1)=IZER(ARG(J))
      BESEL(J,2)=IONE(ARG(J))
      A= -1.
  124 B= -A
      GO TO 123
  118 BESEL(J,1)=YZER(ARG(J))
      BESEL(J,2)=YONE(ARG(J))
      GO TO 120
  119 IF(J-9)121,116,122
  121 BESEL(J,1)=KZER(ARG(J))
      BESEL(J,2)=KONE(ARG(J))
```

```
      A=1.
      B=A
      GO TO 123
  116 BESEL(J,1)=JZER(ARG(J))
      BESEL(J,2)=JONE(ARG(J))
      IF(J-9)120,125,120
  125 BESEL(J,3)=(ARG(J)**2)*(1.-ARG(J)**2/12.)/8.
      BESEL(J,4)=(ARG(J)**3)*(1.-ARG(J)**2/16.)/48.
      GO TO 114
  120 A=1.
      GO TO 124
  122 IF(J-13)115,118,117
  117 IF(J-17)121,116,115
  123 BESEL(J,3)=2.*A*BESEL(J,2)/ARG(J)  +B*BESEL(J,1)
      BESEL(J,4)=4.*A*BESEL(J,3)/ARG(J)  +B*BESEL(J,2)
  114 CONTINUE
      A=-1.
      B=A
      C=-A
      L=1
      M=2
      K=L
  133 DO 130 J=L,M
      COEF(1,J)=A
      COEF(2,J)=B*6.*TERM(J)*AL*CFR(J)
      COEF(3,J)=A*3.*GAM0(K)*AL/ROOT(J)
      COEF(4,J)=A*(3.*SL-ROOT(J))*CFR(J)
      COEF(5,J)=C*TERM(J)*COEF(3,J)/AL
      COEF(6,J)=-B*3.*(SL-ROOT(J))*CFR(J)
      COEF(7,J)=B*9.*TERM(J)*(5.*SL-ROOT(J))*CFR(J)/10.
  130 COEF(8,J)=C*TERM(J)*COEF(6,J)/2.
      IF(M-2)132,132,131
  132 L=5
      K=2
      A=-A
  136 C=-C
      M=L
      GO TO 133
  131 IF(M-5)135,135,134
  135 L=6
      B=-B
      GO TO 136
  134 K=1
      A=-1.
      J=3
  142 COEF(1,J)=0.
      COEF(2,J)=-A*5.*GAM1(K)*(2.*SL-ROOT(J))/(TERM(J)*ROOT(J))
      COEF(3,J)=A
      COEF(4,J)=A*5.*GAM1(K)*AL/ROOT(J)
      COEF(5,J)=-A*AL/TERM(J)
      COEF(6,J)=-COEF(4,J)
      COEF(7,J)=-A*GAM1(K)*AL*(15.*SL-11.*ROOT(J))/(2.*ROOT(J)*TERM(J))
      COEF(8,J)=-TERM(J)*COEF(4,J)/2.
```

```
      COEF(1,J+1)=0.0
      COEF(2,J+1)=-A*2.*AL/TERM(J+1)
      COEF(3,J+1)=0.0
      COEF(4,J+1)=A
      COEF(5,J+1)=0.0
      COEF(6,J+1)=-A*(SL+ROOT(J+1))/(SL-ROOT(J+1))
      COEF(7,J+1)=-A*(3.*SL-ROOT(J+1))/(2.*TERM(J+1))
      COEF(8,J+1)=A*(SL+ROOT(J+1))/(2.*TERM(J+1))
      IF(J-3)141,140,141
  140 J=7
      A=-A
      K=2
      GO TO 142
  141 DO 146 K=5,8
      DO 147 J=1,8
  147 COEF(J,K+4)=COEF(J,K)
      IF(K-5)146,146,148
  148 DO 149 J=2,8,3
  149 COEF(J,K)=-COEF(J,K)
      COEF(7,K)=-COEF(7,K)
  146 CONTINUE
      DO 150 J=1,12
      DO 151 K=1,3,2
  151 T(K,J)=COEF(K,J)*BESEL(J,1)
      T(4,J)=COEF(4,J)*BESEL(J,1)
      DO 152 K=2,5,3
  152 T(K,J)=COEF(K,J)*BESEL(J,2)
      T(6,J)=COEF(6,J)*BESEL(J,3)
      T(7,J)=COEF(7,J)*BESEL(J,2)
  150 T(8,J)=COEF(8,J)*BESEL(J,4)
      DO 155 J=9,12
      DO 155 K=1,4
  155 T(J,K)=0.0
      DO 156 J=5,12
      T(9,J) =COEF(1,J)*BESEL(J+8,1) +2.*COEF(5,J)*BESEL(J+8,2)/3.
      T(9,J) = T(9,J)-(COEF(4,J)*BESEL(J+8,1)-COEF(6,J)*BESEL(J+8,3))/8.
      T(10,J)=2.*COEF(3,J)*BESEL(J+8,1)/3. +COEF(2,J)*BESEL(J+8,2)/4.
      T(11,J)=-COEF(6,J)*BESEL(J+8,3)/48. +8.*COEF(7,J)*BESEL(J+8,2)/21.
      T(11,J)=T(11,J) +(COEF(1,J)/4. +7.*COEF(4,J)/16.)*BESEL(J+8,1)
      T(12,J)=-COEF(1,J)*BESEL(J+8,1)/4. +8.*COEF(8,J)*BESEL(J+8,4)/35.
      T(12,J)=T(12,J) +COEF(4,J)*BESEL(J+8,1)/16.
  156 T(12,J)=T(12,J) +3.*COEF(6,J)*BESEL(J+8,3)/16.
      IF(INDEX(LNC))902,902,352
  902 SUM=CRAM(-12.)
      IF(INDX1(LNC)-1)298,304,313
  298 IF(III)300,300,304
  300 III=1
      PRINT 602, SUM
  602 FORMAT(E16.7,6H = SUM/)
      AL1=AL
      SUM1=SUM
      AL=AL+DL
      GO TO 90
```

```
  304 SLOPE(LNC)=(SUM-SUM1)/(AL-AL1)
      IF(SENSE SWITCH 2)330,313
  330 IF(KKK)314,314,315
  314 KKK=1
      PRINT 604
  604 FORMAT(8X4H SUM,9X6H SLOPE,11X7H LAMBDA/)
  315 PRINT 3,SUM,SLOPE(LNC),AL
  313 SUM1=SUM
      INDX1(LNC)=1
      AL1=AL
      AL=AL-SUM/SLOPE(LNC)
      GO TO 90
  316 PUNCH 604
      PUNCH 3,SUM,SLOPE(LNC),AL1
  352 DO 317 J=1,12
  317 T(J,13)= -T(J,1)
      DO 318 J=1,11
      DO 318 I=1,11
  318 T(J,I)=T(J,I+1)
      DO 319 J=1,11
      T(J,12)=0.
  319 T(12,J)=0.
      X(1)=CRAM(12.)
      IF(SENSE SWITCH 1)932,933
  932 PUNCH 610
  610 FORMAT(5X7H R(I+1)/)
      DO 935 J=1,10
  935 PUNCH 1,X(J)
      PUNCH 2,X(11)
  933 DO 1780 J=1,9
      K8=J +8*(LNC-1)
      K9=J+ 9*(LNC-1)
      IF(J-8)1781,1781,1780
 1781 TEEM(K8)=TERM(J)
 1780 Z(K9)=X(J)
      AAL1(LNC)=AL1
 1800 AAL(LNC)=AL
C
C     COMPUTES LEAST SQUARES ERROR AND STARTS ITERATION ON RF
C
      DO 2101 K=1,NC
      INDEX(K)=0
      INDX1(K)=2
      J=1 +8*(K-1)
      ALSIG(K)=TEEM(J)*SIGF
      BTSIG(K)=TEEM(J+1)*SIGF
      ENSIG(K)=TEEM(J+4)*SIGM
 2101 OMSIG(K)=TEEM(J+5)*SIGM
      DO 235 K=1,NMOD
      IF(R(K)-RF)235,235,236
  235 CONTINUE
  236 NROD=K-1
      DO 2001 J=1,12
```

```
      DO 2001 K=1,13
 2001 T(J,K)=0.
      DO 240 K=1,NC
      DO 240 I=1,NMOD
      L=1+9*(K-1)
      IF(I-NROD)241,241,242
  241 BESEL(I,K)=IZER(ALSIG(K)*R(I)) +Z(L)*IZER(BTSIG(K)*R(I))
      GO TO 240
  242 BESEL(I,K)=Z(L+3)*YZER(ENSIG(K)*R(I))+Z(L+4)*KZER(OMSIG(K)*R(I))
      BESEL(I,K)=BESEL(I,K) +Z(L+7)*JZER(ENSIG(K)*R(I))
      BESEL(I,K)=BESEL(I,K) +Z(L+8)*IZER(OMSIG(K)*R(I))
  240 T(K,13)=T(K,13) +W(I)*BESEL(I,K)*PHI(I)
      DO 244 K=1,NC
      DO 244 J=K,NC
      DO 244 I=1,NMOD
  244 T(K,J)=T(K,J) +W(I)*BESEL(I,J)*BESEL(I,K)
      IF(NC-1)8,245,246
  245 X(1)=T(1,13)/T(1,1)
      GO TO 2248
  246 K2=NC-1
      DO 247 K=1,K2
      K1=K+1
      DO 247 J=K1,NC
  247 T(J,K)=T(K,J)
      NC1=NC+1
      DO 248 J=NC1,12
  248 T(J,J)=1.
      X(1)=CRAM(12.)
 2248 PUNCH 668
  668 FORMAT(2X12H COEFICIENTS)
      DO 2249 J=1,NC
 2249 PUNCH 1,X(J)
      IF(SENSE SWITCH 1)555,5555
  555 PUNCH 667,RF
  667 FORMAT(E16.7,13H = ROD RADIUS/)
      PUNCH 633
  633 FORMAT(1X16H CALCULATED FLUX,5X7H RADIUS/)
 5555 ERR=0.
      DO 2250 I=1,NMOD
      A=0.
      DO 2251 J=1,NC
 2251 A=A +X(J)*BESEL(I,J)
      IF(SENSE SWITCH 1)2520,2250
 2520 PUNCH 7,A,I,R(I)
 2250 ERR=ERR +W(I)*(A-PHI(I))**2
C
C       SWITCH 4 OFF FOR ITERATION ON ROD RADIUS
C
      IF(SENSE SWITCH 4)1200,1199
 1199 IF(MMM-1)1200,1201,1202
 1200 RRF(1)=RF
      EERR(1)=ERR
      PUNCH 666,ERR
```

```
 666 FORMAT(E16.7,8H = ERROR/)
     PUNCH 667,RF
     IF(SENSE SWITCH 4)888,1198
1198 MMM=1
     RF1=RF
     RF=RF +DLTRF
     DO 1900 J=1,NC
     AAL0(J)=AAL(J)
1900 AAL(J)=AAL(J)*(1. +ADD1)
     GO TO 80
1201 MMM=2
     RF1=RF
     RRF(2)=RF
     EERR(2)=ERR
     PUNCH 666,ERR
     PUNCH 667,RF
     RF=RF +DLTRF
1119 DO 1901 J=1,NC
     SLP=(AAL(J)-AAL0(J))/(RRF(2)-RRF(1))
     AAL0(J)=AAL(J)
1901 AAL(J)=AAL(J) +(RF-RRF(2))*SLP
     GO TO 80
1202 RRF(3)=RF
     RF1=RF
     EERR(3)=ERR
     PUNCH 667,RF
     PUNCH 666,ERR
     DO 1907 J=1,12
     DO 1907 K=1,13
1907 T(J,K)=0.
     DO 1908 J=4,12
1908 T(J,J)=1.
     DO 1910 J=1,3
     T(J,1)=1.
     T(J,2)=RRF(J)
     T(J,3)=RRF(J)**2
1910 T(J,13)=EERR(J)
     X(1)=CRAM(12.)
     RF= -X(2)/(2.*X(3))
     PUNCH 667,RF
     DO 1911 J=1,2
     EERR(J)=EERR(J+1)
1911 RRF(J)=RRF(J+1)
     GO TO 1119
1316 PUNCH 666,ERR
     PUNCH 667,RF
     GO TO 8
     END
```

AN INVESTIGATION OF EQUIVALENT RADII FOR P_3 CALCULATIONS IN STRONG ABSORBERS

by

LARRY DEAN NOBLE

B. S., Kansas State University, 1961

AN ABSTRACT OF
A MASTER'S THESIS

submitted in partial fulfillment of the

requirements for the degree

MASTER OF SCIENCE

Department of Nuclear Engineering

KANSAS STATE UNIVERSITY
Manhattan, Kansas

1964

A study is made of the possibility of using a fictional "equivalent rod radius" to accurately predict the neutron flux depression in strong absorbers by the use of the P_3 approximation to the Boltzmann equation for monoenergetic neutron transport.

The theory, appropriate boundary conditions, and the required computer programs were developed for determining the equivalent rod radius from experimental measurements in assemblies having exponential flux dependence in the z- direction. Only cylindrical geometry is considered in the theoretical development.

Application of the commonly applied boundary conditions yielded 16 equations with which to determine 12 unknowns. A study of possible boundary conditions was made, and one combination of 12 equations was found to give a good approximation to the desired physical conditions. It is felt that the same selection rule can be used to determine "correct" boundary conditions for higher order P_L approximations, when L is odd.

Although much of the experimental work is still to be accomplished, the preliminary experimental work performed here strongly indicates that the determination of good "equivalent radii" is entirely feasible.